STEM CELLS®
CANCER STEM CELLS

LGR5-Positive Colon Cancer Stem Cells Interconvert with Drug-Resistant LGR5-Negative Cells and Are Capable of Tumor Reconstitution

SHINTA KOBAYASHI,[a,b] HISAFUMI YAMADA-OKABE,[b] MASAMI SUZUKI,[b] OSAMU NATORI,[a,b] ATSUHIKO KATO,[b] KOICHI MATSUBARA,[a,b] YU JAU CHEN,[a] MASAKI YAMAZAKI,[b] SHINICHI FUNAHASHI,[c] KENJI YOSHIDA,[c] ERI HASHIMOTO,[d] YOSHINORI WATANABE,[d] HIRONORI MUTOH,[d] MOTOOKI ASHIHARA,[d] CHIE KATO,[b] TAKESHI WATANABE,[b] TAKASHI YOSHIKUBO,[b] NORIKAZU TAMAOKI,[e] TAKAHIRO OCHIYA,[f] MASAHIKO KURODA,[g] ARNOLD J. LEVINE,[h] TATSUMI YAMAZAKI[c,i]

[a]PharmaLogicals Research Pte. Ltd., Singapore; [b]Gotemba Research Laboratories, Chugai Pharmaceutical Co., Ltd., Japan; [c]Forerunner Pharma Research Co., Ltd., Japan; [d]Kamakura Research Laboratories, Chugai Pharmaceutical Co., Ltd., Japan; [e]Central Institute for Experimental Animals, Kawasaki, Japan; [f]Division of Molecular and Cellular Medicine, National Cancer Center Research Institute, Tokyo, Japan; [g]Department of Molecular Pathology, Tokyo Medical University, Tokyo, Japan; [h]Institute for Advanced Study, Princeton, New Jersey, USA; [i]Chugai Pharmaceutical Co., Ltd., Japan

Key Words. Cancer stem cells • Drug target • Experimental models • Monoclonal antibodies • Colon cancer • LGR5

ABSTRACT

The cancer stem cell (CSC) concept has been proposed as an attractive theory to explain cancer development, and CSCs themselves have been considered as targets for the development of diagnostics and therapeutics. However, many unanswered questions concerning the existence of slow cycling/quiescent, drug-resistant CSCs remain. Here we report the establishment of colon cancer CSC lines, interconversion of the CSCs between a proliferating and a drug-resistant state, and reconstitution of tumor hierarchy from the CSCs. Stable cell lines having CSC properties were established from human colon cancer after serial passages in NOD/Shi-*scid*, IL-2Rγ^{null} (NOG) mice and subsequent adherent cell culture of these tumors. By generating specific antibodies against LGR5, we demonstrated that these cells expressed LGR5 and underwent self-renewal using symmetrical divisions. Upon exposure to irinotecan, the LGR5$^+$ cells transitioned into an LGR5$^-$ drug-resistant state. The LGR5$^-$ cells converted to an LGR5$^+$ state in the absence of the drug. DNA microarray analysis and immunohistochemistry demonstrated that HLA-DMA was specifically expressed in drug-resistant LGR5$^-$ cells, and epiregulin was expressed in both LGR5$^+$ and drug-resistant LGR5$^-$ cells. Both cells sustained tumor initiating activity in NOG mice, giving rise to a tumor tissue hierarchy. In addition, anti-epiregulin antibody was found to be efficacious in a metastatic model. Both LGR5$^+$ and LGR5$^-$ cells were detected in the tumor tissues of colon cancer patients. The results provide new biological insights into drug resistance of CSCs and new therapeutic options for cancer treatment. STEM CELLS *2012;30:2631–2644*

Disclosure of potential conflicts of interest is found at the end of this article.

INTRODUCTION

Tumors arise from normal tissues by the progression of multiple mutations resulting in malignant cells. The origin of the cells harboring these mutations, whether stem cells (SCs), progenitor cells, or mature differentiated cells, remains unclear. The heterogeneity of tumor cell types and the prevalence of drug resistance have led to the hypothesis for the existence of cancer stem cells (CSCs), although this theory is still an ongoing debate [1–7].

Evidence for the existence of colon CSCs has been the most convincing, with LGR5-positive (LGR5$^+$) cells of particular interest in CSC studies [8–12]. Lgr5, a Wnt target gene, was first identified as a marker for normal SCs in the intestine [13]. It was also reported that Lgr5-positive (Lgr5$^+$) cells formed adenomas upon deletion of Apc and that Lgr5 is expressed in colon cancer cell lines [8]. The cells with high

Authors contributions: H.Y.O and T. Yamazaki: conception and design, data analysis and interpretation, and writing manuscript, and final approval of manuscript; S.K., M.S., O.N., A.K., K.M., and T.O.: collection and assembly of data and data analysis and interpretation; Y.J.C., M.Y., E.H., Y.W., H.M., M.A., C.K., and T.W.: collection and assembly of data; T. Yoshikubo, N.T., and M.K.: data analysis and interpretation; S.F. and K.Y.: provision of study material (new antibodies); A.J.L.: other (support of manuscript). S. K. and H.Y.O. contributed equally to this article.

Correspondence: Hisafumi Yamada-Okabe, Ph.D., Gotemba Research Laboratories, Chugai Pharmaceutical Co., Ltd., 1-135 Komakado, Gotemba, Shizuoka 412-8513, Japan. Telephone: +81-550-87-6709; Fax: +81-550-87-3637; e-mail: okabehsf@chugai-pharm.co.jp Received April 19, 2012; accepted for publication September 1, 2012; first published online in STEM CELLS *EXPRESS* October 18, 2012. 1066-5099/2012/$30.00/0 doi: 10.1002/stem.1257

Wnt activity, thereby rendering them LGR5$^+$, are functionally designated colon CSCs [14]. Clearly, LGR5 is an important molecule to identify colon CSCs.

In the normal intestine, Tian et al. [15] described that Lgr5-negative (Lgr5$^-$) SCs serve as a reserve population of Lgr5$^+$ cells that are themselves therefore dispensable for normal small intestine cell reproduction. It was also reported that slow cycling SCs positive for Hopx are present at the position 4 (the SC crypt), and that there is an interconversion between Hopx$^+$ slow cycling SCs and Lgr5$^+$ proliferating SCs located at the crypt base [16]. Similarly in CSCs, several reports suggest the existence of distinct states of CSCs [17–21]. However, it remains unknown how proliferating CSCs acquire a drug-resistant phenotype and whether interconversion between proliferating and slow cycling/quiescent CSCs occurs. Difficulties in investigating CSCs are due to the heterogeneity of cell types and the rare presence of CSCs in cancer tissues. Many attempts have been made to enrich and isolate CSCs by spheroid cultures in vitro, cell sorting with CSC markers, and direct xenotransplantation of cancer cells to immunodeficient mice [22–30]. Although spheroid cultures enrich CSCs, they result in heterogeneous populations of cells and are not efficient enough to isolate and maintain pure CSC populations [14].

Here we report the establishment of human colon cancer cell lines that express LGR5 and possess CSC properties. The cell lines were created using serial passages of colon cancer cells in xenotransplantion in NOD/Shi-*scid*, IL-2Rγ^{null} (NOG) mice followed by adherent culture of cells. For this purpose, we generated antibodies that are specific to LGR5. The obtained LGR5$^+$ cells transitioned to LGR5-negative (LGR5$^-$) cells upon exposure to an anticancer drug, and such LGR5$^-$ cells reverted to LGR5$^+$ cells after re-seeding and culturing without an anticancer drug. By gene expression profiling of the cell lines, we demonstrated that HLA-DMA, which belongs to the HLA class II alpha chain paralogs, is expressed in drug-resistant LGR5$^-$ cells, and epiregulin (EREG), a member of the epidermal growth factor family, which can function as a ligand of epidermal growth factor receptor and most members of the ErbB family of tyrosine-kinase receptors, is expressed in both proliferating LGR5$^+$ and drug-resistant LGR5$^-$ cells. Using antibodies against LGR5, HLA-DMA, and EREG, we show the existence of LGR5$^+$ and LGR5$^-$ cells in xenotransplanted tumor tissues and in human colon cancer tissues from patients. Furthermore, the anti-EREG antibody exhibited antitumor activity against tumors derived from the LGR5$^+$ cells in a metastatic model. This is the first demonstration of the establishment of stable cell lines having CSC properties and the ability to transition between the two distinct states, a proliferating and a drug-resistant state. Thus, LGR5$^+$ colon CSCs interconvert with drug-resistant LGR5$^-$ cells and are capable of tumor reconstitution. This suggests the physiological importance of CSCs in tumor recurrence after drug treatment. Further, using the anti-EREG antibody, we provide an option for CSC targeting therapy.

Materials and Methods

Preparation of Monoclonal Antibodies Against LGR5

Anti-LGR5 monoclonal antibodies, 2L36 and 2U2E-2, were obtained by DNA immunization and protein immunization, respectively. For DNA immunization, plasmid DNA containing *LGR5* was transferred once a week six times to the abdominal skin of 6-week-old female MRL/lpr mice (MRL/MpJ-Tnfrsf6<lpr>/Crlj). (Charles River Japan, Yokohama, Japan, http://www.crj.co.jp) using a Helicos Gene Gun (Bio-Rad, Hercules, CA, http://www.bio-rad. com) at a pressure of 200–300 psi. At the final immunization, 1×10^6 cells of CHO DG44 (Life Technologies, Rockville, MD, http://www.lifetech.com) expressing LGR5 were intravenously injected. The splenocytes were resected 3 days after the final immunization and fused with P3-X63-Ag8U1 mouse myeloma cells (ATCC, Manassas, VA, http://www.atcc.org). 2L36 was obtained by screening the culture supernatants of hybridoma by flow cytometry [31].

The N-terminal region of LGR5 (amino acid 1–555) was expressed as a fusion protein with the Fc region of mouse IgG2a in CHO DG44 cell. The LGR5-Fc protein secreted in the culture medium was purified with HiTrap Protein A FF column (GE Healthcare, Little Chalfont, United Kingdom, http://www.gehealthcare.com), and then 6-week-old female BALB/c mice (Charles River Japan) were immunized subcutaneously with 50 μg of the LGR5-Fc protein emulsified in Freund's Complete Adjuvant (Becton Dickinson, Franklin Lakes, NJ, http://www.bd.com). Immunization was repeated once a week for 2 weeks with the same amount of the LGR5-Fc protein in Freund's Incomplete Adjuvant (Becton Dickinson). Three days before cell fusion, mice were injected intravenously with 25 μg of the LGR5-Fc protein. Hybridomas were generated as described above, and the antibody 2U2E-2 was selected by ELISA with the LGR5-Fc protein.

Establishment of Human Colon Cancer Xenografts Using NOG Mice

Colon cancer specimens were obtained from consenting patients, as approved by the ethical committee at PharmaLogicals Research and Parkway Laboratory Services in Singapore. Pieces of tumors were minced by scissors and implanted into the flank of NOG mice (Central Institute for Experimental Animals, Kawasaki, Japan, http://www.ciea.or.jp). The human colon cancer xenografts were maintained by passages in NOG mice. All studies and procedures involving animal subjects were approved by the Animal Care and Use Committee at PharmaLogicals Research and the Institutional Animal Care and Use Committee at Chugai Pharmaceutical Co., Ltd. The animals used in this experiment were treated in accordance with the Animal Research Guideline of PharmaLogicals Research and the Guidelines for the Care and Use of Laboratory Animals at Chugai Pharmaceutical Co., Ltd.

Establishment of Colon Cancer Cell Lines with CSC Properties

Single cell suspension of cancer cells from the xenografts was prepared by mincing the tissues with scissors, incubated in Dulbecco's phosphate buffered saline (DPBS) containing collagenase/dispase (Roche, Basel, Switzerland, http://www.roche-applied-science.com) and DNase I (Roche) at 37°C for 3 hours followed by filtrating 40 μm cell strainer (BD Biosciences, San Diego, CA, http://www.bdbiosciences.com) and suspending in lysing buffer (BD Biosciences). The cells were cultured in a SC medium [Dulbecco's modified Eagle's medium/F12 medium (Life Technologies) supplemented with N-2 supplement (Life Technologies), 20 ng/ml human epidermal growth factor (Life Technologies), 10 ng/ml human basic fibroblast growth factor (Sigma-Aldrich, St. Louis, MO, http://www.sigmaaldrich.com), 4 μg/ml heparin (Sigma-Aldrich), 4 mg/ml bovine serum albumin (BSA) (Life Technologies), 20 μg/ml human insulin, zinc solution (Life

Technologies), and 2.9 mg/ml glucose (Sigma-Aldrich)] at 37°C under 5% CO_2 [32]. Culture flasks treated with polystyrene (BD Biosciences) and ultra-low-attachment cell culture flasks (Corning Life Sciences, Acton, MA, http://www.corning.com/lifesciences) were used for adherent cultures and the spheroid cultures, respectively. Drug-resistant $LGR5^-$ cells were obtained by treating the adherent $LGR5^+$ cells with 10 μg/ml irinotecan (Hospira, Lake Forest, IL, http://www.hospira.com/) for 3 days.

Sorting of the $LGR5^+$ and $LGR5^-$ Cells

The primary cells from xenografts were incubated with the anti-LGR5 antibody (2L36, 2 μg/ml) and then R-phycoerythrin (PE)-labeled anti-mouse IgG2a (Life Technologies, 1/200 dilution). Mouse cells were discriminated from the human colon cancer cells by staining with anti-mouse major histocompatibility complex (MHC) class I antibody (Abcam, Cambridge, U.K., http://www.abcam.com, 0.1 μg/ml) and allophycocyanin (APC)-labeled anti-rat IgG (BioLegend, San Diego, CA, http://www.biolegend.com, 1/100 dilution). Anti-CD133 antibody (Miltenyi Biotec, Bergisch Gladbach, Germany, http://www.miltenyibiotec.com, 5 μg/ml) and Alexa 488-labeled anti-mouse IgG1 (Life Technologies, 1/100 dilution) were used to detect CD133. Dead cells were removed by 7- aminoactinomycin D (7-AAD) viability dye (Beckman Coulter, Brea, CA, http://www.beckmancoulter.com). Flow cytometry analysis and cell sorting were performed using a MoFlo XDP (Beckman Coulter) cell sorter.

In Vitro Colony Formation Assay

To test the colony formation ability, cells were seeded on a layer of 100% Matrigel (BD Biosciences) at 10,000 cells per well and cultured in a SC medium supplemented with 10% heat-inactivated fetal bovine serum (FBS) and 5% Matrigel.

Tumor Formation In Vivo

Cells suspended in Hank's balanced salt solution (Life Technologies) with 50% Matrigel were subcutaneously inoculated into the flank of NOG mice. For single cell inoculation, cells were stained with fluorescein isothiocyanate (FITC)-labeled anti-EpCAM antibody (Miltenyi Biotec) and seeded in Terasaki plates (Thermo Fisher Scientific, Waltham, MA, http://www.thermofisher.com). After the presence of single cell in each well was confirmed under a fluorescence microscope, the single cell in 50 μl of 50% Matrigel was inoculated into the flank of mice. Estimated CSC density was calculated by the formula available on the WEHI ELDA website [33].

Histological Examination

Small pieces of surgical specimens of human tissues and of the xenograft tumor tissues were fixed with 4% paraformaldehyde at 4°C for 16–24 hours and embedded in paraffin by the AMeX method [34, 35]. After washing the in vitro cultured cells with phosphate buffered saline (PBS)-EDTA, the cells were fixed with 4% paraformaldehyde at 4°C for 2 hours, suspended in 0.5 ml agarose, and embedded in paraffin with AMeX method. Thin sections were subjected to hematoxylin & eosin staining and to immunohistochemisty.

Immunohistochemistry

Thin sections from the above-mentioned paraffin blocks were incubated with anti-LGR5 antibody (2U2E-2, 1 μg/ml), anti-EREG antibody (10 μg/ml), anti-E-cadherin antibody (Abcam, 2.5 μg/mL), anti-HLA-DMA antibody (Sigma-Aldrich, 2.5 μg/ml), or FITC-labeled anti-Ki67 antibody (Abcam, 2.5 μg/mL). After the incubation with the primary antibodies, the sections were incubated with a secondary antibody conjugated with polymer-horseradish peroxidase (HRP) (DAKO, Glostrup, Denmark, http://www.dako.com or Vector Laboratories, Burlingame, CA, http://www.vector labs.com) or biotin, and the proteins were visualized by AlexaFluor 488-labeled tyramide (Life Technologies, 1/100 dilution), AlexaFluor 568-labeled tyramide (Life Technologies, 1/100 dilution), or AlexaFluor 568-labeled streptavidin (Life Technologies, 2 μg/ml). For immunofluorescent cytochemistry, cells were fixed with 4% paraformaldehyde and permeabilized with 0.1% Triton-X 100 (Sigma-Aldrich), and incubated with anti-LGR5 antibody (2L36, 2 μg/ml). After the incubation with the primary antibodies, the cells were incubated with AlexaFluor 488-labeled anti-mouse IgG (Life Technologies, 1/100 dilution). Those specimens and cells were also stained with DAPI (Life Technologies).

Induction of the Transition Between $LGR5^+$ and $LGR5^-$ States in Single Cell Culture

$LGR5^+$ cells were sorted with an anti-LGR5 antibody, and single $LGR5^+$ cells were cultured in 96-well microplates. To obtain drug-resistant $LGR5^-$ cells, $LGR5^+$ cells were treated with 10 μg/ml irinotecan for 3 days. Single $LGR5^-$ cells were cultured in 96-well microplates for 4 days. The medium used for the single cell culture contained 10% conditioned medium of the in vitro cultured $LGR5^+$ cells under an adherent condition. $LGR5^+$ and $LGR5^-$ states of the cells were confirmed by immunocytochemical analysis with anti-LGR5 antibody.

Determination of Antitumor Activity of Anti-EREG Antibody In Vivo

2×10^6 of $LGR5^+$ cells were suspended in Hank's balanced sodium solution and intravenously injected into the tail vein of Fox Chase severe combined immunodeficiency (SCID) Beige Mouse (CB17.Cg-Prkdc^{scid}Lyst^{bg}/Crl, Charles River Japan). For treatment with the anti-EREG antibody, the mice were intravenously administered 10 mg/kg of anti-EREG antibody once a week for five times starting 3 days after tumor inoculation. Mice were scarified 5 days after the final administration under deep anesthesia, and lung tissues were collected. The lung tissues trimmed into 11 pieces were fixed in 4% paraformaldehyde for 24 hours, paraffin embedded by AMeX method [34, 35]. After thin sections were prepared and stained with hematoxylin & eosin, the number of tumors was counted. The sizes of the tumors were determined under a microscope with micrometer.

Statistical Analysis

The Mann–Whitney *U* test was applied to determine the statistical significance of the differences in the numbers of tumor nodules in a metastatic tumor model. The statistical analysis was carried out with an SAS preclinical package (SAS Institute, Inc., Cary, NC, http://www.sas.com). *p* values smaller than 0.05 were considered significant.

Results

Generation and Characterization of Specific Antibodies Against LGR5

Having an antibody specific to LGR5 is critical to isolate and characterize colon CSCs, but such antibody has not been available yet. Therefore, we first attempted to generate anti-LGR5 antibodies that enable us to isolate and analyze cells having colon CSC properties. Two monoclonal antibodies, 2L36 and 2U2E-2, specific to LGR5 were obtained. The regions of the LGR5 protein that contain epitopes of these

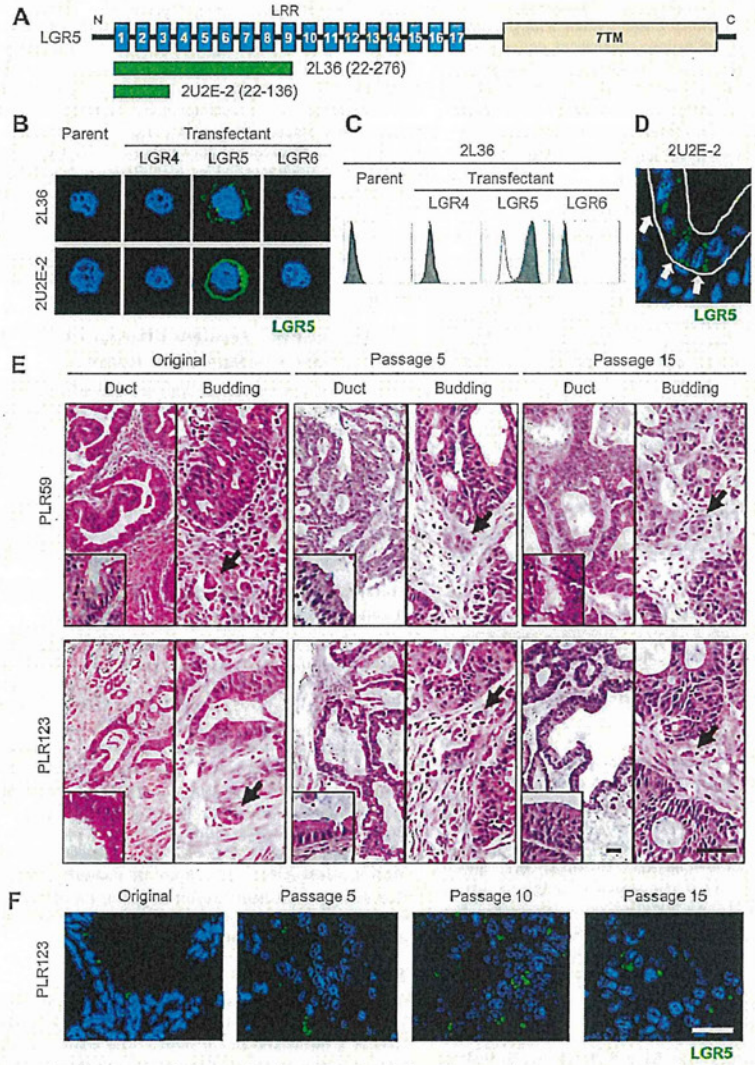

Figure 1. Antigen-specific binding of anti-LGR5 antibodies and characteristics of human colon cancer xenografts using NOG mice. **(A):** Regions of the LGR5 protein that contain epitopes of the anti-human LGR5 monoclonal antibodies, 2L36 and 2U2E-2. The monoclonal antibodies, 2L36 and 2U2E-2, were obtained by immunizing the *LGR5* cDNA and N-terminal region of the protein, respectively. Green bars correspond to the regions containing epitopes. **(B, C):** Specific binding of the anti-LGR5 antibodies to the antigen. (B): Immunocytochemistry of CHO DG44 cells transfected with the *LGR4*, *LGR5*, or *LGR6* cDNA. 2L36 and 2U2E-2 recognized the cells expressing LGR5 but not those expressing LGR4 or LGR6. (C): Flow cytometry analysis of CHO DG44 cells transfected with the *LGR4*, *LGR5*, or *LGR6* cDNA. 2L36 reacted with the cells expressing LGR5 but not those expressing LGR4 or LGR6. **(D):** Staining of the crypt base cells in normal human intestine. The thin sections of the normal human intestine were stained with 2U2E-2. Specific fluorescence was observed in the crypt base columnar cells (arrows). **(E):** Histology of surgically resected tumors of PLR59 and PLR123 and xenograft tumor tissues. Tumors derived from PLR59 and PLR123 had tubular structures containing goblet cells (inserts) and budding cluster (arrows). Bar = 50 μm. **(F):** Immunostaining of LGR5 in the surgically resected tumors (PLR123) and xenografts derived from PLR123. Sections were stained with the anti-LGR5 antibody. Bar = 25 μm. Original, surgically resected tumors from patients.

antibodies are shown in Figure 1A. Both antibodies were tested for immunohistochemistry and flow cytometry using the CHO cells expressing highly related proteins LGR4, LGR5, or LGR6. When used for immunostaining, both 2L36 and 2U2E-2 recognized CHO cells expressing LGR5 but not those expressing LGR4 or LGR6 (Fig. 1B). In flow cytometry analysis, only 2L36 strongly reacted with CHO cells expressing LGR5 (Fig. 1C). Moreover, the antibody 2U2E-2 reacted specifically with crypt base columnar cells in the normal human intestine (Fig. 1D; Supporting Information Fig. S1A).

There was also a good correlation between mRNA expression and cell surface staining of the anti-LGR5 antibody in human colon cancer cell lines, which included the CSC lines established in this study and six commercially available lines (Supporting Information Fig. S1B).

Establishment of Human Colon Cancer Cell Lines with CSC Properties

We established 11 human colon cancer xenografts using NOG mice [36]. Ten out of 11 xenografts were derived from moderately differentiated colon cancer, and one was from poorly differentiated colon cancer. Both the moderately differentiated colon cancer xenografts and the poorly differentiated colon cancer xenograft reconstituted almost the same histological morphologies as the original tumors; the moderately differentiated colon cancer xenografts formed clear epithelial ducts and small budding clusters. In contrast, the poorly differentiated colon cancer xenograft showed no clear epithelial duct structure. We used two moderately differentiated colon cancer xenografts, namely PLR59 and PLR123, for the establishment of colon CSC lines. PLR59 and PLR123 were heterozygous for the mutant K-Ras (G12D), and PLR123 carried the mutant p53 (R249M) in one allele. These xenografts were chosen because they grew faster while retaining the ability to reconstitute tumors with epithelial ducts and small budding clusters even after 10 passages in NOG mice (Fig. 1E). In the epithelial ducts of the tumors, differentiated cancer cells that showed goblet cell-like phenotype were also observed in the xenotransplanted tumor tissues throughout the passages (Fig. 1E, inset).

To confirm the existence of CSCs in the xenotransplanted tumor tissues, we used immunohistochemical staining for the LGR5 protein that marks colon CSCs. $LGR5^+$ cells were detected in the original tumor tissues of PLR59 and PLR123 and in their xenotransplanted tumor tissues throughout the passages (Fig. 1F). The frequency of $LGR5^+$ cells in the original tumor tissues was quite low: it was approximately 0.01% in PLR59 and approximately 0.04% in PLR123. In the xenotransplanted tumor tissues, the frequency of $LGR5^+$ cells increased during the passages (Fig. 1F). Tumor initiating activity (TIA) of the primary cells from the PLR123 xenografts was also increased after the passages. The estimated percentage of CSC in the primary cells, as judged from TIA, was approximately 0.1% after five passages, and after 14 passages it increased to approximately 0.4% (Supporting Information Table S1). Schematic representation of the establishment of the colon cancer cell lines is shown in Figure 2A.

CSC Properties of the Established Colon Cancer Cell Lines

The major properties of CSCs are self-renewal, TIA, and the reconstitution of a tumor tissue hierarchy of differentiated cells. In an attempt to establish cell lines possessing CSC properties, we used spheroid and adherent cultures of the cells derived from PLR59 and PLR123 xenografts in which $LGR5^+$ cells were enriched (over 10 passages). When cells derived from PLR59 and PLR123 were cultured as spheroids, their growth was rather slow, and the spheroids contained only a few $LGR5^+$ cells but more differentiated cells that were positive for CK20, which is a commonly used differentiation marker (Supporting Information Fig. S2). On the contrary, cells from PLR59 and PLR123 cultured under an adherent condition grew fast with a doubling time of approximately 2.5 days and showed epithelial morphology (Fig. 2B).

To examine TIA of the cells, subcutaneous injection of 10 cells from the spheroids formed tumors in one (PLR59-derived cells) or two (PLR123-derived cells) out of six injection sites (Supporting Information Table S2), whereas 10 cells from adherent cultures formed tumors in all six injection sites, and even a single cell injection of an adherent cell reconstituted tumors. Although the spheroid culture led to an increase in TIA as compared to that of the primary cells, the adherent culture was more efficiently enriched in cells possessing TIA. The histological morphology of the tumors from the adherent cells was almost the same as the original tumors (Fig. 2C). In addition, TIA of the adherent cells was maintained even after the cells were cultured for more than a month (Supporting Information Table S3).

We examined cell surface markers of the adherent cells from the PLR59 and PLR123 and found that they were clearly positive for all known colon CSC markers reported earlier: $LGR5^+$, $ALDH^+$, $CD133^+$, $CD44^+$, $EpCAM^+$, $CD166^+$, $CD24^+$, $CD26^+$, and $CD29^+$ (Fig. 2D; Supporting Information Fig. S3). In addition, expression of the cell surface markers was unchanged even after 1 month of cell culture. One of the characteristics of CSCs is symmetrical cell division for self-renewal. The $LGR5^+$ adherent cells divided symmetrically under the adherent culture conditions (Fig. 2E). In the presence of Matrigel and FBS, however, the $LGR5^+$ cells underwent asymmetrical cell divisions, as demonstrated by the segregation of LGR5 protein into one of two daughter cells (Fig. 2F), implicating the generation of two different offspring. Asymmetric cell divisions are one of the hallmarks of SCs.

Colony Forming Activity and Tumorigenicity of the Sorted $LGR5^+$ and the $LGR5^-$ Cells

In order to examine the ability of $LGR5^+$ and $LGR5^-$ cells to form colonies in vitro and tumors in vivo, we sorted the $LGR5^+$ and $LGR5^-$ populations from the primary cells of xenografts generated by the inoculation of the $LGR5^+$ cells. Anti-LGR5 antibody 2L36 was used for the cell sorting. About 93% of the cells in the $LGR5^+$ fraction were $LGR5^+$, and more than 99% of the cells in the $LGR5^-$ fraction were $LGR5^-$ (Fig. 3A). The sorted $LGR5^+$ cells but not the $LGR5^-$ cells efficiently formed colonies on Matrigel in vitro and formed tumors in NOG mice. When 1,000 cells were subcutaneously injected into NOG mice, the sorted $LGR5^+$ cells formed large visible tumors by day 34 after the inoculation, but the $LGR5^-$ cells gave rise to only very tiny tumors by day 34 (Fig. 3B). We further examined the relation of LGR5 expression and other CSC markers by double staining the LGR5 with CD133, CD166, or CD44. Nearly all of the $LGR5^+$ cells were positive for CD133 and CD166, but there were large numbers of $LGR5^-$ cells that were positive for CD133 or CD166, indicating that LGR5 marks a subpopulation of $CD133^+$ and $CD166^+$ cells (Fig. 3C). Because significant numbers of $LGR5^+/CD44^-$ cells were present, CD44 does not mark all the $LGR5^+$ cells (Fig. 3C).

We used cell sorting to further characterize the $LGR5^-$ cell populations. The cells from the xenografts were stained with the anti-LGR5 and anti-CD133 antibodies, and the $LGR5^-/CD133^-$, $LGR5^{-/low}/CD133^+$, and $LGR5^+/CD133^+$ cells were separated. More than 90% of the cells in each fraction were $LGR5^-/CD133^-$, $LGR5^{-/low}/CD133^+$, and $LGR5^+/CD133^+$ (Fig. 3D). The isolated $LGR5^+/CD133^+$ and $LGR5^{-/low}/CD133^+$ cells formed colonies on Matrigel, whereas nearly all the $LGR5^-/CD133^-$ cells died after seeding on culture plates; colony forming efficiency of the sorted $LGR5^-/CD133^-$, $LGR5^{-/low}/CD133^+$, and $LGR5^+/CD133^+$ cells were about 0.03%, 1.6%, and 4.3%, respectively (Fig. 3E; Supporting Information Fig. S4).

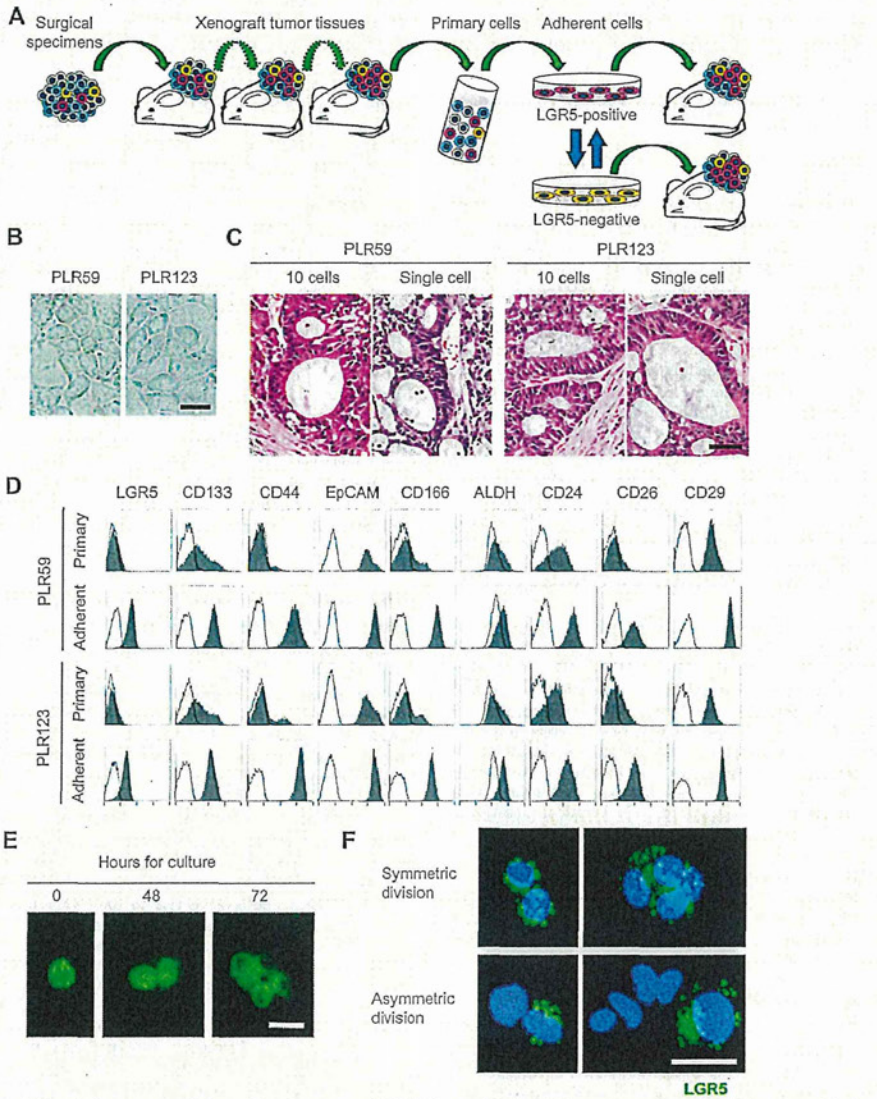

Figure 2. Characteristics of colon cancer cell lines with cancer stem cell (CSC) properties. **(A):** Schematic representation of the process for the establishment of colon cancer cell lines. **(B):** Phase contrast microscopy of the cells in the LGR5$^+$ cell lines. Cells were collected from xenografts of PLR59 and PLR123 after more than 10 passages in NOD/Shi-*scid*, IL-2Rγ^{null} (NOG) mice and cultured under an adherent culture condition. Bar = 20 μm. **(C):** Histology of the tumors derived from the LGR5$^+$ cells from PLR59 and PLR123 xenografts. Ten or single LGR5$^+$ cells from the adherent cultures of the cells derived from PLR59 and PLR123 xenografts were subcutaneously injected into NOG mice. Bar = 50 μm. **(D):** Expression of CSC markers. The primary cells from xenografts of PLR59 and PLR123 after more than 10 passages in NOG mice (upper) and the LGR5$^+$ cells cultured under an adherent culture condition (lower) were analyzed by flow cytometry. Shadow, Fluorescent intensities after staining with the indicated antibodies or ALDH activity; Open, Fluorescent intensities after staining with control isotype antibody or ALDH activity with an ALDH inhibitor. **(E):** Symmetric division of the LGR5$^+$ cells. The LGR5$^+$ cells stained with PKH67 dye were cultured for 72 hours and examined by fluorescent microscopy. Bar = 20 μm. **(F):** Symmetrical (upper) and asymmetrical (lower) divisions of the LGR5$^+$ cells in the presence or absence of Matrigel and fetal bovine serum. Photographs of the cells were taken after single division (left) and after two or three divisions (right). The LGR5$^+$ cells were cultured for 48–72 hours and stained with the anti-LGR5 antibody. Bar = 20 μm.

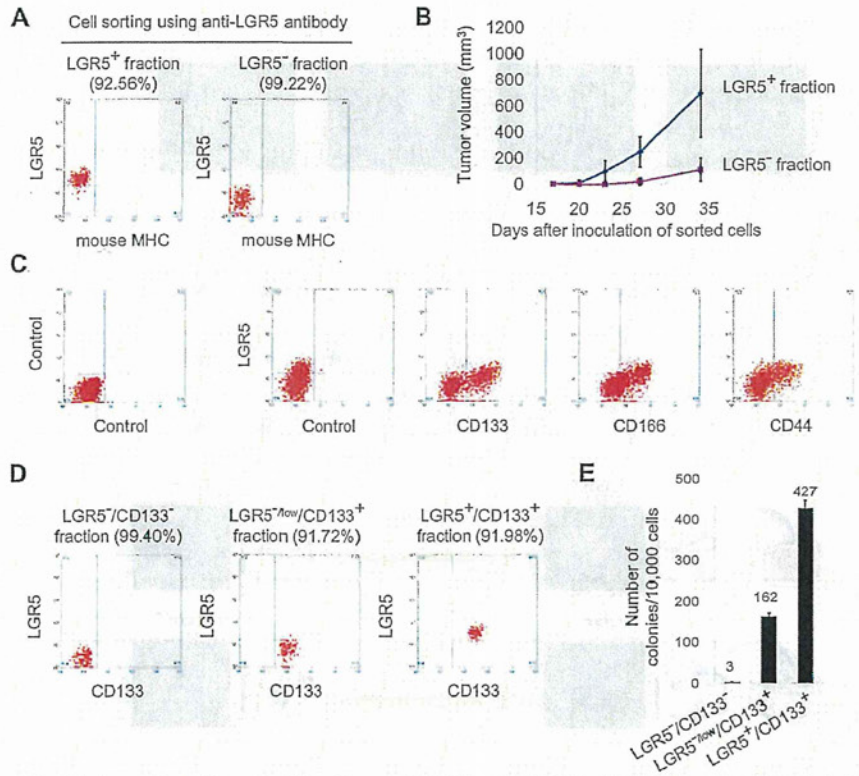

Figure 3. Colony forming activity and tumorigenicity of the sorted LGR5$^+$ and the LGR5$^-$ cells. **(A):** Flow cytometry analysis of the sorted LGR5$^+$ and LGR5$^-$ populations from the primary cells of PLR123 xenograft generated by the inoculation of the LGR5$^+$ cells. Percentages indicate the purity of the sorted cell population. **(B):** Tumor formation by the sorted LGR5$^+$ and the LGR5$^-$ cells. One thousand cells of the sorted LGR5$^+$ and the LGR5$^-$ populations suspended in Matrigel were subcutaneously inoculated into NOG mice, and tumor volume was measured. Mean ± SD of six tumors is shown. **(C):** Flow cytometry analysis of the primary cells from the PLR123 xenograft after staining with anti-LGR5 antibody together with anti-CD133, anti-CD166, or anti-CD44 antibody. **(D):** Flow cytometry analysis of the cells in the sorted LGR5$^-$/CD133$^-$, LGR5^{-low}/CD133$^+$ and LGR5$^+$/CD133$^+$ populations from the primary cells of the PLR123 xenograft. Percentages indicate the purity of the sorted cell population. **(E):** Colony forming activity of the sorted LGR5$^-$/CD133$^-$, LGR5^{-low}/CD133$^+$ and LGR5$^+$/CD133$^+$ cells. Ten thousand cells of the sorted cells were seeded on Matrigel. Number of colonies after culturing the cells for 6 days was determined. Mean ± SD in triplicate experiments is shown.

Interconversion Between LGR5$^+$ Proliferating and LGR5$^-$ Drug-Resistant States

We next asked whether the LGR5$^+$ cells exhibited a drug-resistant state, which is believed to be a typical characteristic of CSCs [37]. After treatment of the LGR5$^+$ cells with irinotecan for 3 days, the cells stopped proliferation and about half of the cells survived (Supporting Information Fig. S5). One hundred percent of the surviving cells became LGR5$^-$, but they retained other colon CSC markers (Fig. 4A, 4B; Supporting Information Fig. S6, Table S4). The LGR5$^-$ cells induced by treating the LGR5$^+$ cells with an anticancer drug were designated as drug-resistant LGR5$^-$ cells in this study. LGR5$^-$ cells which were pre-existing in xenograft tissues and human tumor tissues are referred to as LGR5$^-$ cells. Reverse transcriptase real-time polymerase chain reaction (RT-qPCR) for *LGR5*, *CD133*, *CD44*, *CD166*, and *EPCAM* revealed that the *LGR5* mRNA was drastically decreased after irinotecan treatment, but the mRNAs of *CD133*, *CD44*, *CD166*, and *EPCAM* did not decline or even increased after treatment (Supporting Information Fig. S7D). The mRNA level of *CK20* did not increase by the irinotecan treatment and remained at a low level (Supporting Information Fig. S2A). Although we cannot rule out the possibility that elimination of epitope by proteolytic cleavage on LGR5 occurred after irinotecan treatment, the cells that were not recognized by any of our anti-LGR5 antibodies were regarded as LGR5 negative. We examined the TIA of these drug-resistant LGR5$^-$ cells. Even injection of the 10 LGR5$^-$ cells formed tumors in two sites (PLR59-derived cells), and the PLR123-derived cells formed tumors at one site out of six injection sites in the NOG mice (Supporting Information Table S5). Treatment of the LGR5$^+$ cells with 5-fluorouracil or oxaliplatin also gave rise to drug-resistant LGR5$^-$ cells which converted to an LGR5$^+$ state after re-seeding and culturing in the absence of the drugs (Supporting Information Fig. S8).

The drug-resistant LGR5$^-$ cells did not grow even after irinotecan was removed from the culture medium

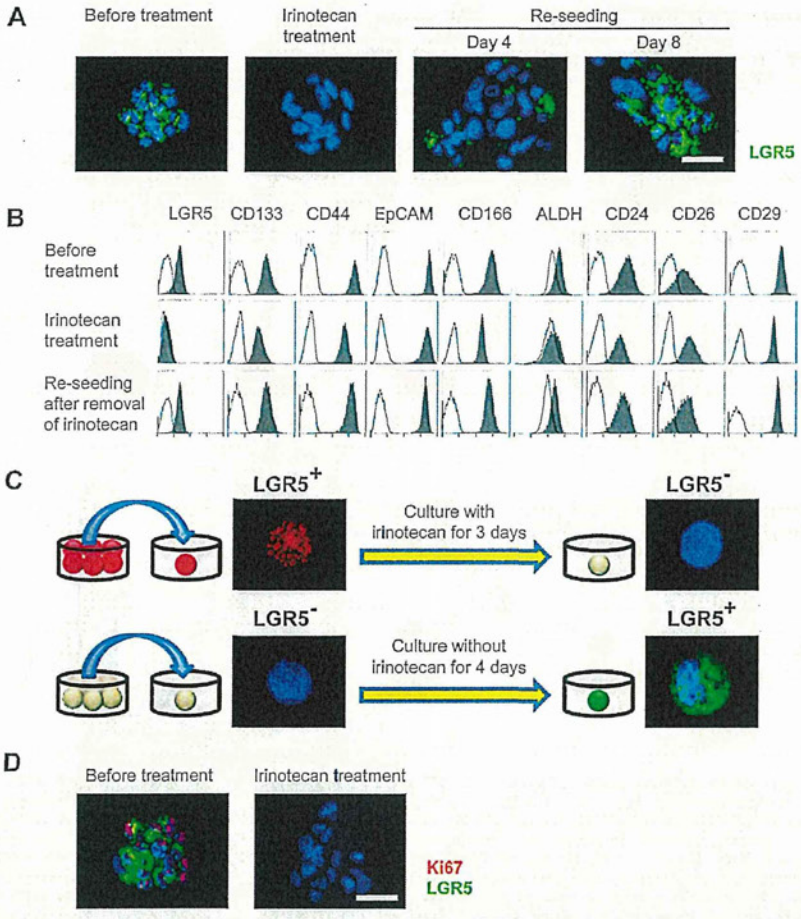

Figure 4. Transition of the colon cancer stem cells (CSCs) between LGR5$^-$ and LGR5$^-$ states in vitro. **(A):** Immunostaining of LGR5 after treatment of the LGR5^l cells with irinotecan. The adherent LGR5^l cells from PLR123 xenografts cultured in the presence of irinotecan became LGR5$^-$. The drug-resistant LGR5$^-$ cells were re-seeded and further cultured in the absence of irinotecan for the indicated days. The LGR5$^+$ cells appeared 4 days after the reseeding and increased by 8 days. Bar = 50 μm. **(B):** Expression of CSC markers. The LGR5$^+$ cells from the adherent cultures from PLR123 xenografts before (top) and after treatment with irinotecan (middle) were analyzed by flow cytometry. Cells re-seeded after irinotecan treatment (bottom) were also analyzed. Shadow, Fluorescent intensities after staining with the indicated antibodies or ALDH activity; Open, Fluorescent intensities after staining with control isotype antibody or ALDH activity with an ALDH inhibitor. **(C):** Interconversion of the LGR5$^+$ and LGR5$^-$ states in vitro. LGR5$^+$ cells collected by flow cytometry were seeded by limiting dilutions and cultured under an adherent culture condition in the presence of irinotecan for 3 days. Drug-resistant LGR5$^-$ cells that had been treated with irinotecan were seeded by limiting dilutions and cultured under an adherent culture condition for 4 days. The cells were stained with anti-LGR5 antibody to confirm the expression of LGR5. LGR5 was visualized by R-phycoerythrin (PE)-labeled anti-mouse IgG (red) or by AlexaFluor 488-labeled anti-mouse IgG (green). **(D):** Ki67 staining of the LGR5$^+$ and drug-resistant LGR5$^-$ cells. In vitro cultures of the LGR5$^+$ cells and the drug-resistant LGR5$^-$ cells obtained by the treatment of the adherent LGR5$^+$ cells with irinotecan were double stained with the anti-LGR5 antibody and an anti-Ki67 antibody. Bar = 50 μm.

(Supporting Information Fig. S5C). However, they became positive for LGR5 and resumed proliferation after replating (Fig. 4A, 4B). The transition from the LGR5$^+$ state to an LGR5$^-$ state and vice versa was also confirmed by observations with single cells in culture. When single LGR5$^+$ cells were cultured in multiwell plates, the cells transitioned to an LGR5$^-$ state within 3 days after irinotecan treatment. When single LGR5$^-$ cells that had been treated with irinotecan were then cultured in multiwell plates without irinotecan, 19%–43% of the cells converted to the LGR5$^+$ state within 4 days (Fig. 4C; Supporting Information Table S6). In order to confirm proliferation of the LGR5$^+$ and drug-resistant LGR5$^-$ cells, we also used double staining of LGR5 and Ki67 with the in vitro cultures of the LGR5$^+$ and the LGR5$^-$ cells. The expression of LGR5 correlated well with Ki67 staining: the LGR5$^+$ cells were positive for Ki67, and the drug-resistant LGR5$^-$ cells were negative for Ki67 (Fig. 4D).

Pathway analysis using the results of DNA microarray of both proliferating LGR5$^+$ and drug-resistant LGR5$^-$ cells revealed characteristics of two distinct states. As expected from the growth status of the cells, genes involved in cell cycle were downregulated whereas genes in the p53 signaling pathway were upregulated in the drug-resistant LGR5$^-$ cells (Supporting Information Fig. S9). Genes whose mRNA expression increased in the LGR5$^+$ cells included those involved in cell growth such as *LGR5*, *FGFBP1*, *FGFR4*, *ROR1*, *NFIA*, *PIGU*, *LPAR3*, and *FZD2* (Supporting Information Fig. S7C).

Reconstitution of the Epithelial Cell Type Tumor Hierarchy from LGR5$^+$ Cells

The observations that the cells converted from the LGR5$^+$ to the drug-resistant LGR5$^-$ state in vitro and that the drug-resistant LGR5$^-$ cells formed tumors in vivo prompted us to examine whether the drug-resistant LGR5$^-$ cells directly generate a tumor hierarchy of differentiated cell types or first convert to the LGR5$^+$ state in vivo. To detect drug-resistant LGR5$^-$ cells, we attempted to identify the genes that are upregulated in the drug-resistant LGR5$^-$ cells by comparing the gene expression profiles of the drug-resistant LGR5$^-$ cells, the LGR5$^+$ cells, and the primary cells from the xenografts. From the gene expression analyses of DNA microarray, a heat map is shown (Fig. 5A; Supporting Information Fig. S7) for the top 20 genes encoding membrane proteins with the largest change. Genes whose mRNA expression was increased in the drug-resistant LGR5$^-$ cells include MHC class II-related genes (*HLA-DMA*, *HLA-DMB*), adhesion molecule-related genes (*AMIGO2*, *FLRT3*, *GJB5*, *CLDN1*), G-protein-coupled receptor protein signaling pathway-related genes (*GPR87*, *GPR110*, *GPR172B*, *GNAI1*, *ABCA1*), and immune signaling-related genes (*TNFSF15*, *BLNK*, *FAS*, *TMEM173*). We further evaluated the genes for which antibodies against their proteins are available (Supporting Information Table S7).

Immunohistochemical staining of the cells cultured in vitro with antibodies confirmed that HLA-DMA was rather specifically expressed in the drug-resistant LGR5$^-$ cells (Fig. 5B). HLA-DMA was located in intracellular vesicles, and therefore, it cannot be used for cell sorting. Nevertheless, HLA-DMA can be a useful molecule for identifying the LGR5$^-$ cells in xenografts and in clinical specimens. Because HLA-DMA is also expressed in macrophages, we looked for genes that were expressed in both LGR5$^+$ and drug-resistant LGR5$^-$ cells and identified EREG (Fig. 5A). Immunohistochemical staining with a monoclonal antibody against EREG confirmed the EREG expression in LGR5$^+$ and LGR5$^-$ cells (Fig. 5B; Supporting Information Fig. S10). By combination of these markers, LGR5$^-$ cells can be detected as HLA-DMA and EREG double positive cells. After injection of a homogenous population of drug-resistant LGR5$^-$ cells into NOG mice, cells weakly expressing LGR5 but still positive for HLA-DMA and EREG appeared within 1 day after the injection, and then the LGR5$^+$/EREG$^+$ cells which were negative for HLA-DMA emerged by day 5 (Fig. 5C). The reconstitution of the epithelial tumor hierarchy of diverse cell types from the drug-resistant LGR5$^-$ cells through transition to LGR5$^+$ cells was confirmed (Fig. 5D).

We next examined the possibility of a conversion of LGR5$^+$ cells to a drug-resistant state in vivo. NOG mice bearing tumors derived from the LGR5$^+$ cells were administered intraperitoneally with a maximum tolerated dose (MTD) dose (120 mg/kg) of irinotecan. Tumor growth was nearly completely inhibited (Fig. 5E), and ductal structures were heavily destroyed (Fig. 5F). Under such conditions, the LGR5$^+$ cells were markedly decreased (Fig. 5F; Supporting Information Fig. S11). There was a significant increase in HLA-DMA-positive cells, which are LGR5$^-$, after irinotecan treatment. In contrast, about one-third of the cancer cells in both ducts and budding regions were LGR5$^+$ in the vehicle-treated control mice. Both LGR5$^+$ cells and HLA-DMA$^+$/LGR5$^-$ cells were positive for EREG (Fig. 5F). The LGR5$^+$ cells reappeared after termination of irinotecan treatment (Fig. 5F; Supporting Information Fig. S11). We also performed double staining with Ki67 and LGR5 or HLA-DMA that marks LGR5$^-$ CSCs. As in the in vitro cultured cells, there was a good correlation of LGR5 expression and Ki67 staining of the cells in the xenografts. The LGR5$^+$ cells were positive for Ki67, and the LGR5$^-$/HLA-DMA$^+$ cells were negative for Ki67 (Fig. 5G). Thus, tumor reconstitution occurred through the LGR5$^+$ cells.

Possible Therapeutic Application of Anti-EREG Antibody

EREG is expressed on the surface of both LGR5$^+$ and drug-resistant LGR5$^-$/HLA-DMA$^+$ cells, but its expression is very low or hardly detectable in differentiated tumor cells and normal tissues (Fig. 5A; Supporting Information Fig. S12A). Therefore, EREG may be a potential therapeutic target. We first examined the growth inhibitory activity and antibody dependent cell cytotoxicity (ADCC) activity of the anti-EREG antibody. The anti-EREG antibody induced ADCC activity against both LGR5$^+$ and drug-resistant LGR5$^-$ cells in the presence of human peripheral blood mononuclear cells (PBMC) that contained effector cells, such as natural killer (NK) cells and monocytes, but the antibody did not directly affect the growth of LGR5$^+$ and drug-resistant LGR5$^-$ cells in the absence of effector cells in vitro (Supporting Information Fig. S12B, S12C). To test the expression of EREG in vivo, we subcutaneously inoculated the LGR5$^+$ cells into NOG mice in which EREG was highly expressed during early stages of tumor development, and later its expression was rather restricted to budding areas as compared to ducts when tumors formed clear duct structures. EREG-positive cells were also detected after the mice bearing the tumors were administered irinotecan (Fig. 5F). Therefore, we tested the antitumor activity of the anti-EREG antibody after irinotecan treatment. SCID mice were used as a model for efficacy evaluation, because the antibody requires effector cells to elicit ADCC. When the antibody was administered at day 4 and day 11 after the final administration of irinotecan, it only delayed the tumor growth (Supporting Information Fig. S12D).

To test the efficacy in a metastatic model, we first examined the expression of EREG in metastasized tumors. When the LGR5$^+$ cells were intravenously injected into NOG mice, tumors were developed in several organs including the lung. For the tumors that developed in the lung, the majority of tumor cells were EREG positive (Fig. 6A). Efficacy was then tested using SCID-Beige mice in which macrophages and monocytes can serve as effectors for ADCC. When the antibody was administered once a week for five times starting 3 days after the tumor injection, the number of tumors at different sites was significantly decreased as compared to the control mice (Fig. 6B). In addition, the size of each tumor was also markedly reduced in the antibody treated mice (Fig. 6C, 6D).

The Existence of Both LGR5$^+$ and LGR5$^-$ Cells in Human Colon Cancers

We asked whether LGR5$^+$ and LGR5$^-$ cells could be detected in tissue sections of clinical colon cancers. Although rare, the LGR5$^+$ cells and the LGR5$^-$ cells which were HLA-DMA$^+$/EREG$^+$ were present in primary and metastatic colon cancer tissues from patients (Fig. 7A). Among 12 human

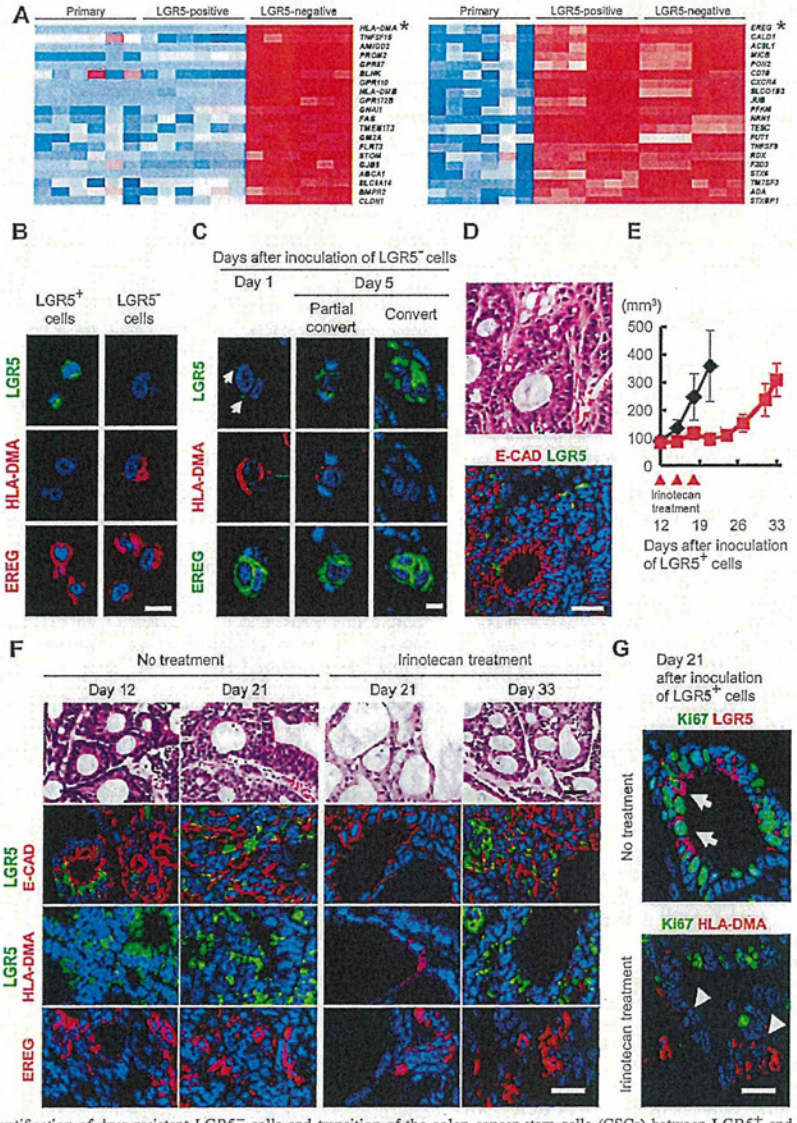

Figure 5. Identification of drug-resistant LGR5$^-$ cells and transition of the colon cancer stem cells (CSCs) between LGR5$^+$ and LGR5$^-$ states in vivo. **(A):** DNA microarray. RNA prepared from the primary cells from xenografts, LGR5$^+$ cells, and drug-resistant LGR5$^-$ cells derived from PLR59 and PLR123 were analyzed by Affymetrix U133. Heat map of 20 genes whose expression was markedly upregulated in the drug-resistant LGR5$^-$ cells as compared to the LGR5$^+$ cells (left) and that of 20 genes whose expression was increased in both LGR5$^+$ and drug-resistant LGR5$^-$ cells as compared to the primary cells from the xenografts (right) are shown. **(B):** Expression of HLA-DMA and EREG in LGR5$^+$ and drug-resistant LGR5$^-$ cells. The LGR5$^+$ (left) and drug-resistant LGR5$^-$ cells (right) derived from PLR123 xenografts were stained with anti-LGR5 antibody (top), anti-HLA-DMA antibody (middle), and anti-EREG antibody (bottom). Bar = 10 μm. **(C):** Transition from drug-resistant LGR5$^-$ cells to LGR5$^+$ cells during the early process of tumor development. The drug-resistant LGR5$^-$ cells derived from PLR123 xenografts were injected into NOG mice, and the tumors derived from the drug-resistant LGR5 cells were stained with anti-LGR5, anti-HLA-DMA, and anti-EREG antibodies. Arrow: Weakly staining of LGR5 on Day 1. Two typical types of cells are shown. Partial convert: Moderate staining of LGR5 with weakly staining of HLA-DMA on Day 5. Convert: Strong staining of LGR5 with no staining of HLA-DMA on Day 5. Bar = 10 μm. **(D):** Reconstitution of tumor hierarchy from the drug-resistant LGR5$^-$ cells. Histology (upper) and immunostaining with the anti-LGR5 and E-cadherin antibodies (lower) are shown. Bar = 50 μm. **(E):** Tumor volume of the xenografts. The LGR5$^+$ cells of PLR123 were subcutaneously injected into NOG mice, and the mice were administered irinotecan (120 mg/kg per day) 12, 15, and 18 days after the inoculation of the tumor cells. Tumor volume of the control mice (black line) and that of the mice which received irinotecan (red line) are shown. Each value represents mean ± SD (n = 5). **(F):** Histology and immunostaining for LGR5, HLA-DMA, and EREG of the tumors after treatment of irinotecan. Sections of the xenografts in (E) were excised from the mice at the indicated days after the inoculation of the LGR5$^+$ cells and stained with H&E, anti-LGR5 antibody, anti-HLA-DMA antibody, or anti-EREG antibody. Bar = 25 μm. **(G):** Ki67 staining of the LGR5$^+$ and the HLA-DMA$^+$ cells in xenografts. The sections of the xenografts excised from the mice 21 days after the inoculation of the LGR5$^+$ cells with or without treatment of irinotecan were double stained with anti-Ki67 antibody and anti-LGR5 antibody or anti-HLA-DMA antibody. Arrows: LGR5$^+$/Ki67$^+$ cells, arrow heads: HLA-DMA$^+$/Ki67$^-$ cells. Bar = 25 μm. Abbreviation: EREG, epiregulin.

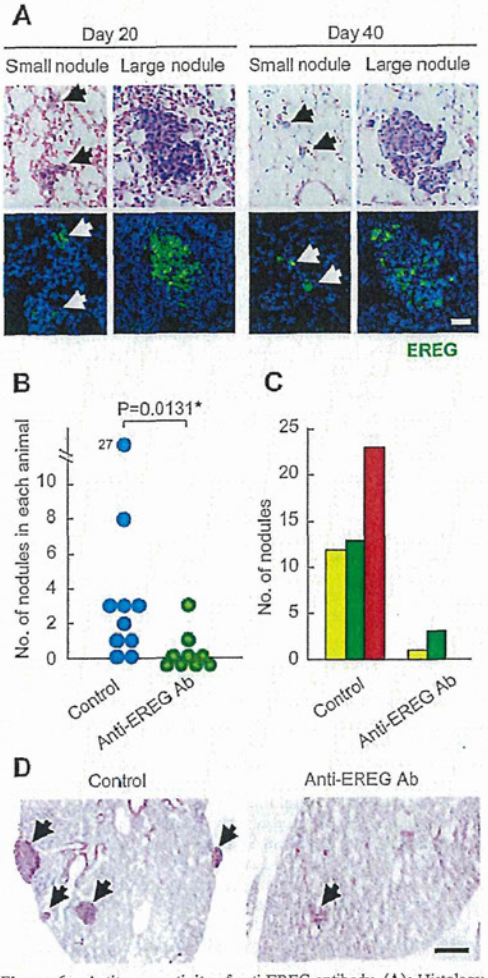

Figure 6. Antitumor activity of anti-EREG antibody. (A): Histology (upper) and immunostaining for EREG (lower) of the tumors. The adherent LGR5$^+$ cells derived from PLR123 xenografts were intravenously injected into NOD/Shi-*scid*, IL-2Rγ^{null} (NOG) mice. Tumors were dissected on the indicated days after inoculation of tumor cells. Photographs of typical large and small nodules are shown. Bar = 50 μm. (B–D): Numbers and histology of tumors in lung. Severe combined immunodeficiency (SCID)-Beige mice were intravenously injected with the adherent LGR5$^+$ cells derived from PLR123 xenografts. The anti-EREG antibody was administered every week for five times starting from 3 days after the tumor inoculation. Lung of the animals were resected and examined histologically with 11 cross-sections of the lung per animal (n = 10 for control group and n = 9 for anti-EREG antibody injected group). Number of tumor nodules per animal is shown in (B). Each symbol represents individual animal. Total numbers of tumor nodules in each group of the mice with the indicated sizes are shown in (C). Yellow column; under 100 μm, green column; 100–200 μm, red column; over 200 μm. Histology of the tumors with or without administration of anti-EREG antibody are shown in (D). Bar = 200 μm. Abbreviation: EREG, epiregulin.

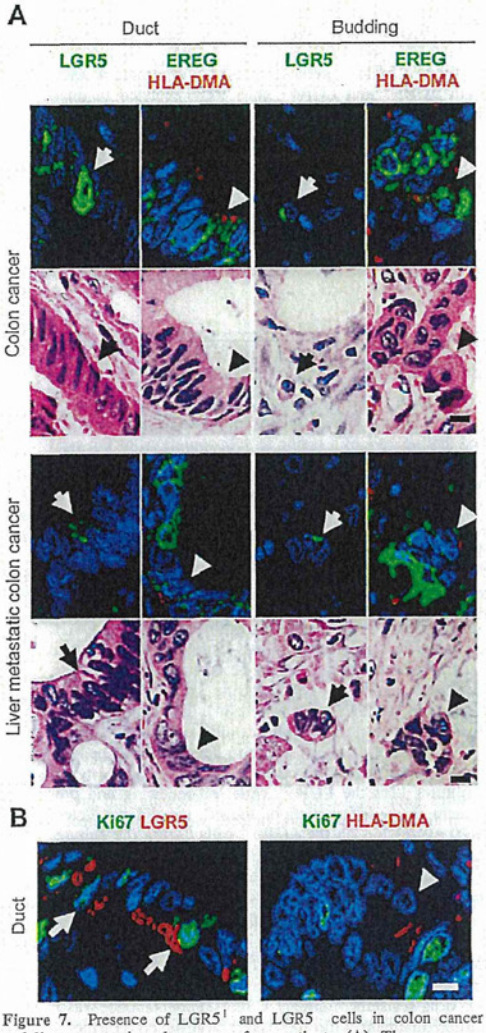

Figure 7. Presence of LGR5$^+$ and LGR5$^-$ cells in colon cancer and liver metastatic colon cancer from patients. (A): The same section of the primary and liver metastatic colon cancer tissues from patients was stained with H&E or antibodies against LGR5, HLA-DMA, and EREG. LGR5$^+$ and EREG$^+$/HLA-DMA$^+$ cells are detected in both ductal structures and budding areas of the primary and liver metastatic tumors. LGR5$^+$ cells present as a single cell are also found in the interstitium. Similar patterns of the staining were observed in several tumor tissues from different patients. Arrows indicate typical LGR5$^+$ cells, and arrow heads indicate typical LGR5$^-$/EREG$^+$/HLA-DMA$^+$ cells. Bar = 10 μm. (B): Ki67 staining of the LGR5$^+$ and the HLA-DMA$^+$ cells in colon cancer tissues from patients. The sections of the primary colon cancer tissues from patients in (A) were double stained with an anti-Ki67 antibody and anti-LGR5 antibody or anti-HLA-DMA antibody. Arrows: LGR5$^+$/Ki67$^+$ cells, Arrow head: HLA-DMA$^+$/Ki67$^-$ cells. Bar = 10 μm. Abbreviation: EREG, epiregulin.

colon cancer tissues, both $LGR5^+$ cells and $LGR5^-$ cells were detected in eight cases, and either $LGR5^+$ or $LGR5^-$ cells were observed in the remaining four cases. The percentages of the $LGR5^+$ and $LGR5^-$ cells in those cases ranged between 0.003% and 1.864% for the $LGR5^+$ and 0.001%–0.243% for the $LGR5^-$ cells (Supporting Information Table S8). Both $LGR5^+$ and $LGR5^-$ cells were detected in ducts and budding areas (Fig. 7A; Supporting Information Table S8). In addition, $LGR5^+$ and $LGR5^-$ cells within the ducts were not restricted to particular regions as they were observed randomly throughout the ducts (Fig. 7A). In budding areas, $LGR5^+$ cells were detected as a single cell or in tumor cell clusters consisting of a few tumor cells (Fig. 7A). Also in clinical specimens, the $LGR5^+$ cells were positive for Ki67, and the $LGR5^-$/HLA-DMA$^+$ cells were negative for Ki67 (Fig. 7B).

Discussion

SC markers such as CD133, CD44, CD166, and ALDH have been used to identify and isolate colon CSCs [25–29]. We observed that colon CSCs reside in subpopulations of the cells positive for these markers; however, none is a definitive marker for colon CSCs. Evidence that Lgr5 marks normal intestinal SCs has accumulated [8, 13]. Despite that evidence, LGR5 remains unexplored in human CSCs, presumably due to a lack of specific antibodies [38]. In this study, we generated monoclonal antibodies that are highly specific to LGR5 and can be applied to immunostaining, flow cytometry, and cell sorting. Using these unique anti-LGR5 antibodies, we were able to define $LGR5^+$ cells as proliferating colon CSCs. To establish pure CSC cell lines, we tested whether spheroid cultures or adherent cultures would be useful to enrich CSCs. Several attempts have been made using spheroid cultures to isolate and enrich CSCs in vitro [9, 14]. The results in this study indicated that spheroid cultures allowed $LGR5^+$ cells to self-renew and differentiate, leading to heterogeneous populations of cells as reported by others [14, 39]. In contrast, adherent cultures kept the $LGR5^+$ cells self-renewing and prevented them from differentiation. Indeed, we did not detect any CK20 expression on the $LGR5^+$ cells during the culture. Thus, the $LGR5^+$ cell lines form a highly homogenous population of cells having CSC properties with strong TIA. Only a few previous reports have described the use of adherent cultures to obtain CSCs such as in glioma and breast cancers [30, 40, 41]. The adherent cultures were rehighlighted to isolate stable cell lines with CSC properties in this study.

Using the established $LGR5^+$ cell lines, definitive evidence for drug-resistant $LGR5^-$ CSC subpopulations was obtained after treatment with anti-cancer drugs such as irinotecan. The $LGR5^+$ cells had a number of CSC characteristics such as self-renewal via symmetric and asymmetric division, TIA, and a pathway for producing a tumor hierarchy of different cell types. In addition, these cell lines transition between two distinct states, an $LGR5^+$ proliferating and an $LGR5^-$ drug-resistant state. Tumor formation from the drug-resistant $LGR5^-$ cells in NOG mice was observed, but the TIA of the drug-resistant $LGR5^-$ cells was slightly lower than that of $LGR5^+$ cells. Drug-resistant $LGR5^-$ cells first converted to $LGR5^+$ cells in the establishment of tumor hierarchy in vivo. The results of irinotecan treatment in vivo suggest that anti-cancer drugs induce transition of $LGR5^+$ cells to drug-resistant cells, and such drug-resistant cells revert to $LGR5^+$ cells after drug treatment is terminated. We could detect both $LGR5^+$ and $LGR5^-$ cells in ducts and budding sites of the tumors reconstituted from either the $LGR5^-$ or $LGR5^+$ cells in mice and also in primary and liver metastasized tumors from patients. These observations may explain why some rare populations of CSCs survive after drug treatments, giving rise to tumor recurrence. If this idea is correct, the CSC cell lines provide a new avenue to test drugs that will kill all of the cancer cells in a tumor.

CSCs self-renew and also give rise to differentiated cancer cells. In fact, the $LGR5^+$ cells exhibited the ability to undergo asymmetric cell divisions, generating two different offspring in vitro and reconstituting tumor hierarchy in vivo. However, it remains unclear whether a transition of differentiated cancer cells to CSCs occurs. Gupta et al. [20] proposed a stochastic state transition of cancer cells. Using breast cancer cell lines, they demonstrated that differentiated cancer cells possessed plasticity and transitioned to CSCs to maintain phenotypic proportions within tumors, although the frequency was very low (between 0.01% and 0.1%). In this study, the colony forming activity of the sorted cells in the 99.4% pure $LGR5^-$/$CD133^-$ population, in which almost all the cells are CSC marker-negative and thereby considered to be differentiated tumor cells, was approximately 0.03%. This number is extremely low but not zero. Therefore, the possibility of a reversion of differentiated cells to CSCs, as proposed by Gupta et al., cannot be ruled out. At the same time, the possibility that colonies were formed by a small number of concomitant $LGR5^+$ cells in this faction also cannot be excluded. Further study which overcomes technological hurdles of cell sorting is necessary to answer this question.

In normal small intestine, the existence of two types of SCs has been described: slow cycling SCs in the +4 position and proliferating SCs in the crypt base [42]. However, the relationship between the two types of SCs was unclear. More recently, $Lgr5^-$/$Bmi1^+$ SCs were shown to serve as a SC pool: they changed to $Lgr5^+$ SCs when the $Lgr5^+$ SCs were absent [15]. Furthermore, Takeda et al. [16] demonstrated the interconversion and bidirectional lineage relationship between proliferating $Lgr5^+$ SCs at the crypt base column and slow cycling SCs that expressed an atypical homeobox protein Hopx at +4 position. Tert, telomerase reverse transcriptase, was reported as molecules that mark predominately noncycling, long-lived intestinal SCs that proliferate upon injury [43]. Powell et al. [44] also demonstrated that expression of Lrig1, a pan ErbB inhibitor, was rather specific to quiescent SCs. However, Wong et al. [45] indicated the coexpression of Lrig1 in $Lgr5^+$ cells, and intensive analysis with DNA microarray and proteomics revealed that Bmi1, Tert, Hopx and Lrig1 were all robustly expressed in $Lgr5^+$ intestinal SCs [46]. In our RT-qPCR analysis, the *HOPX* mRNA was not detected in the $LGR5^+$ and drug-resistant $LGR5^-$ cells, whereas similar levels of the *BMI1* and *LRIG1* mRNA were detected in both $LGR5^+$ and drug-resistant $LGR5^-$ states (Supporting Information Fig. S13). In addition, expression of *TERT* was rather specific to the $LGR5^+$ cells; there was a marked decrease of the *TERT* mRNA after the $LGR5^+$ cells were treated with irinotecan (Supporting Information Fig. S13), which coincided with the results that intestinal SCs contained significant telomerase activity [47]. Except for *HOPX* mRNA expression, we observed expression of the *BMI1*, *LRIG1*, and *TERT* mRNAs in proliferating colon CSCs. Definitive understanding of the physiological roles and the expression of these genes in normal and cancer SCs await further study.

Because localization of proliferating ($Lgr5^+$) and slow cycling quiescent ($Lgr5^-$) SCs is restricted in normal intestine as described above, localization, proliferation, and transition between the slow cycling and proliferating states of SCs may be controlled by niches which include a gradient of the Wnt ligand [42]. The moderately differentiated colon cancers differed from the normal architecture: it showed duct structures

and an epithelial hierarchy, but localization of $LGR5^+$ and $LGR5^-$ cells in ducts appeared not to be restricted to particular regions in both xenotransplanted tumors and in colon cancer tissues in patients, and they were observed throughout ducts. Thus, it seems that in tumor tissues, CSCs undergo proliferation and interconversion of their states without the underlying architecture of gradient producing cells at specific locations in the tissue structure.

It is widely believed that the invasive ability of cancer cells is important for metastasis. In addition, tumor budding is suggested to contribute to metastasis in colon cancer [48]. We could identify three markers—LGR5, HLA-DMA, and EREG—that can mark these CSCs in two distinct states. Because both proliferating and drug-resistant colon CSCs were EREG positive, we addressed whether anti-EREG antibody is efficacious against tumor metastasis. The antibody showed only moderate activity against the established xenograft tumors but exhibited a stronger efficacy in a metastatic model tested in this study, suggesting that the anti-EREG antibody is efficacious in the early stage of cancer development when cancers are rich in CSCs. A number of studies suggest that metastatic nodules arise from rare cells in the primary tumor (CSCs) [49]. If this is correct, then therapies targeting CSCs can have profound effects against metastatic tumors, even greater than upon primary tumors. In this way, the CSC cell lines developed here can give rise to novel therapies that could improve the treatment of cancer patients.

During the review process for this article, three papers appeared providing the evidence for the existence of CSCs in solid tumors in mice: Chen J. et al. (Nature 2012: 488: 522-526), Driessens G. et al. (Nature 2012: 488: 527-530), and Schepers AG et al. (Science 2012: 337: 730-735).

Conclusion

We established human colon cancer cell lines that express LGR5 and possess CSC properties. After treatment of the proliferating $LGR5^+$ cells with an anticancer agent, the $LGR5^+$ cells transition to a drug-resistant $LGR5^-$ state. In addition, the $LGR5^-$ cells converted to an $LGR5^+$ state in the absence of the drug, suggesting a pool of SCs with the ability to interconvert between two distinct states. Using antibodies against LGR5, HLA-DMA, and EREG, we show the existence of $LGR5^+$ and $LGR5^-$ cells in xenotransplanted tumor tissues and in human colon cancer tissues from patients. Furthermore, the anti-EREG antibody exhibited antitumor activity against tumors derived from the $LGR5^+$ cells in a metastatic model. This suggests the physiological importance of CSCs in tumor recurrence. Furthermore, using the anti-EREG antibody, we provide an option for CSC targeting therapy.

Acknowledgments

We thank L.C. Wong, G.N. Yeow, H.S. Ong, Z.X. Wong, and Y. Takai for their technical assistance; Y. Ohnishi, E. Fujii, K. Nakano, Y. Hirata, and K.F-Ouchi for critical discussions; and R. Somerville for proof editing the manuscript. Thanks are also to T. Yamamura and R. Nomura for their continuous support throughout the study. We are also grateful to O. Nagayama, Chairman and CEO of Chugai, for his encouragement. This work is supported in part by a grant from Singapore Economic Development Board.

Disclosure of Potential Conflicts of Interest

S.K., H.Y.O., M.S., O.N., A.K., K.M., M.Y., S.F., K.Y., E.H., Y.W., H.M., M.A., C.K., T.W., T.Yo, and T.Ya. are employees of Chugai Pharmaceutical Co., Ltd. Y.J.C. is employee of PharmaLogicals Research Pte. Ltd. The authors indicate no other potential conflict of interest.

References

1 Shackleton M, Quintana E, Fearon ER et al. Heterogeneity in cancer: Cancer stem cells versus clonal evolution. Cell 2009;138:822–829.
2 Clevers H. The cancer stem cell: Premises, promises and challenges. Nat Med 2011;17:313–319.
3 Vaiopoulos AG, Kostakis ID, Koutsilieris M et al. Concise review: Colorectal cancer stem cells. Stem Cells 2012;30:363–371.
4 Nguyen LV, Vanner R, Dirks P et al. Cancer stem cells: An evolving concept. Nat Rev Cancer 2012;12:133–143.
5 Marusyk A, Almendro V, Polyak K. Intra-tumour heterogeneity: A looking glass for cancer? Nat Rev Cancer 2012;12:323–334.
6 Visvader JE, Lindeman GJ. Cancer stem cells: Current status and evolving complexities. Cell Stem Cell 2012;10:717–728.
7 Magee JA, Piskounova E, Morrison SJ. Cancer stem cells: Impact, heterogeneity, and uncertainty. Cancer Cell 2012;21:283–296.
8 Barker N, Ridgway RA, van Es JH et al. Crypt stem cells as the cells-of-origin of intestinal cancer. Nature 2009;457:608–611.
9 Vermeulen L, Todaro M, de Sousa Mello F et al. Single-cell cloning of colon cancer stem cells reveals a multi-lineage differentiation capacity. Proc Natl Acad Sci USA 2008;105:13427–13432.
10 Takahashi H, Ishii H, Nishida N et al. Significance of Lgr5(+ve) cancer stem cells in the colon and rectum. Ann Surg Oncol 2011;18:1166–1174.
11 Takeda K, Kinoshita I, Shimizu Y et al. Expression of LGR5, an intestinal stem cell marker, during each stage of colorectal tumorigenesis. Anticancer Res 2011;31:263–270.
12 Walker F, Zhang HH, Odorizzi A et al. LGR5 is a negative regulator of tumourigenicity, antagonizes Wnt signalling and regulates cell adhesion in colorectal cancer cell lines. PLoS One 2011;6:e22733.
13 Barker N, van Es JH, Kuipers J et al. Identification of stem cells in small intestine and colon by marker gene Lgr5. Nature 2007;449:1003–1007.
14 Vermeulen L, De Sousa E Melo F, van der Heijden M et al. Wnt activity defines colon cancer stem cells and is regulated by the microenvironment. Nat Cell Biol 2010;12:468–476.
15 Tian H, Biehs B, Warming S et al. A reserve stem cell population in small intestine renders Lgr5-positive cells dispensable. Nature 2011;478:255–259.
16 Takeda N, Jain R, LeBoeuf MR et al. Interconversion between intestinal stem cell populations in distinct niches. Science 2011;334:1420–1424.
17 Quintana E, Shackleton M, Foster HR et al. Phenotypic heterogeneity among tumorigenic melanoma cells from patients that is reversible and not hierarchically organized. Cancer Cell 2010;18:510–523.
18 Sharma SV, Lee DY, Li B, at al. A chromatin-mediated reversible drug-tolerant state in cancer cell subpopulations. Cell 2010;141:69–80.
19 Roesch A, Fukunaga-Kalabis M, Schmidt EC et al. A temporarily distinct subpopulation of slow-cycling melanoma cells is required for continuous tumor growth. Cell 2010;141:583–594.
20 Gupta PB, Fillmore CM, Jiang G et al. Stochastic state transitions give rise to phenotypic equilibrium in populations of cancer cells. Cell 2011;146:633–644.
21 Dieter SM, Ball CR, Hoffmann CM et al. Distinct types of tumor-initiating cells form human colon cancer tumors and metastases. Cell Stem Cell 2011;9:357–365.
22 Lapidot T, Sirard C, Vormoor J et al. A cell initiating human acute myeloid leukaemia after transplantation into SCID mice. Nature 1994;367:645–648.
23 Al-Hajj M, Wicha MS, Benito-Hernandez A et al. Prospective identification of tumorigenic breast cancer cells. Proc Natl Acad Sci USA 2003;100:3983–3988.

24 Singh SK, Hawkins C, Clarke ID et al. Identification of human brain tumour initiating cells. Nature 2004;432:396–401.
25 O'Brien CA, Pollett A, Gallinger S et al. A human colon cancer cell capable of initiating tumour growth in immunodeficient mice. Nature 2007;445:106–110.
26 Ricci-Vitiani L, Lombardi DG, Pilozzi E et al. Identification and expansion of human colon-cancer-initiating cells. Nature 2007;445: 111–115.
27 Dalerba P, Dylla SJ, Park IK et al. Phenotypic characterization of human colorectal cancer stem cells. Proc Natl Acad Sci USA 2007; 104:10158–10163.
28 Huang EH, Hynes MJ, Zhang T et al. Aldehyde dehydrogenase 1 is a marker for normal and malignant human colonic stem cells (SC) and tracks SC overpopulation during colon tumorigenesis. Cancer Res 2009;69:3382–3389.
29 Chu P, Clanton DJ, Snipas TS et al. Characterization of a subpopulation of colon cancer cells with stem cell-like properties. Int J Cancer 2009;124:1312–1321.
30 Mather JP. Concise Review: Cancer stem cells: In vitro models. Stem Cells 2012;30:95–99.
31 Kremer L, Marquez G. Generation of monoclonal antibodies against chemokine receptors. Methods Mol Biol 2004;239:243–260.
32 Todaro M, Alea MP, Di Stefano AB et al. Colon cancer stem cells dictate tumor growth and resist cell death by production of interleukin-4. Cell Stem Cell 2007;1:389–402.
33 Hu Y, Smyth GK. ELDA: Extreme limiting dilution analysis for comparing depleted and enriched populations in stem cell and other assays. J Immunol Methods 2009;347:70–78.
34 Sato Y, Mukai K, Watanabe S et al. The AMeX method. A simplified technique of tissue processing and paraffin embedding with improved preservation of antigens for immunostaining. Am J Pathol 1986;125: 431–435.
35 Suzuki M, Katsuyama K, Adachi K et al. The combination of fixation using PLP fixative and embedding in paraffin by the AMeX method is useful for histochemical studies in assessment of immunotoxicity. J Toxicol Sci 2002;27:165–172.
36 Fujii E, Suzuki M, Matsubara K et al. Establishment and characterization of in vivo human tumor models in the NOD/SCID/gamma(c) (null) mouse. Pathol Int 2008;58:559–567.
37 Buczacki S, Davies RJ, Winton DJ. Stem cells, quiescence and rectal carcinoma: An unexplored relationship and potential therapeutic target. Br J Cancer 2011;105:1253–1259.
38 Barker N, Bartfeld S, Clevers H. Tissue-resident adult stem cell populations of rapidly self-renewing organs. Cell Stem Cell 2010;7:656–670.
39 Emmink BL, Van Houdt WJ, Vries RG et al. Differentiated human colorectal cancer cells protect tumor-initiating cells from irinotecan. Gastroenterology 2011;141:269–278.
40 Pollard SM, Yoshikawa K, Clarke ID et al. Glioma stem cell lines expanded in adherent culture have tumor-specific phenotypes and are suitable for chemical and genetic screens. Cell Stem Cell 2009;4: 568–580.
41 Scheel C, Eaton EN, Li SH et al. Paracrine and autocrine signals induce and maintain mesenchymal and stem cell states in the breast. Cell 2011;145:926–940.
42 Li L, Clevers H. Coexistence of quiescent and active adult stem cells in mammals. Science 2010;327:542–545.
43 Montgomery RK, Carlone DL, Richmond CA et al. Mouse telomerase reverse transcriptase (mTert) expression marks slowly cycling intestinal stem cells. Proc Natl Acad Sci USA 2011;108:179–184.
44 Powell AE, Wang Y, Li Y et al. The pan-ErbB negative regulator Lrig1 is an intestinal stem cell marker that functions as a tumor suppressor. Cell 2012;149:146–158.
45 Wong VW, Stange DE, Page ME et al. Lrig1 controls intestinal stem-cell homeostasis by negative regulation of ErbB signaling. Nat Cell Biol 2012;14:401–408.
46 Muñoz J, Stange DE, Schepers AG et al. The Lgr5 intestinal stem cell signature: Robust expression of proposed quiescent '+4' cell markers. EMBO J 2012;31:3079–3091.
47 Schepers AG, Vries R, van den Born M et al. Lgr5 intestinal stem cells have high telomerase activity and randomly segregate their chromosomes. EMBO J 2011;30:1104–1109.
48 Brabletz T, Jung A, Spaderna S et al. Opinion: Migrating cancer stem cells—An integrated concept of malignant tumour progression. Nat Rev Cancer 2005;5:744–749.
49 Wu X, Northcott PA, Dubuc A et al. Clonal selection drives genetic divergence of metastatic medulloblastoma. Nature 2012;482:529–533.

See www.StemCells.com for supporting information available online.

Systemically Injected Exosomes Targeted to EGFR Deliver Antitumor MicroRNA to Breast Cancer Cells

Shin-ichiro Ohno[1], Masakatsu Takanashi[1], Katsuko Sudo[2], Shinobu Ueda[1], Akio Ishikawa[1], Nagahisa Matsuyama[1], Koji Fujita[1], Takayuki Mizutani[1], Tadaaki Ohgi[3], Takahiro Ochiya[4], Noriko Gotoh[5] and Masahiko Kuroda[1]

[1]Department of Molecular Pathology, Tokyo Medical University, Tokyo, Japan; [2]Animal Research Center, Tokyo Medical University, Tokyo, Japan; [3]BONAC Corporation, Fukuoka BIO Factory 4F, Fukuoka, Japan; [4]Division of Molecular and Cellular Medicine, National Cancer Center Research Institute, Tokyo, Japan; [5]Division of Systems Biomedical Technology, Institute of Medical Science, University of Tokyo, Tokyo, Japan

Despite the therapeutic potential of nucleic acid drugs, their clinical application has been limited in part by a lack of appropriate delivery systems. Exosomes or microvesicles are small endosomally derived vesicles that are secreted by a variety of cell types and tissues. Here, we show that exosomes can efficiently deliver microRNA (miRNA) to epidermal growth factor receptor (EGFR)-expressing breast cancer cells. Targeting was achieved by engineering the donor cells to express the transmembrane domain of platelet-derived growth factor receptor fused to the GE11 peptide. Intravenously injected exosomes delivered let-7a miRNA to EGFR-expressing xenograft breast cancer tissue in RAG2$^{-/-}$ mice. Our results suggest that exosomes can be used therapeutically to target EGFR-expressing cancerous tissues with nucleic acid drugs.

Received 17 March 2012; accepted 1 August 2012; advance online publication 2 October 2012. doi:10.1038/mt.2012.180

INTRODUCTION

MicroRNAs (miRNAs) are small (20–22 nucleotides) noncoding RNA molecules that bind to partially complementary mRNA sequences, resulting in target degradation or translation inhibition.[1] A growing pool of evidence suggests that miRNA-related gain- or loss-of-function mutations can cause the development and/or progression of cancer.[2] For example, let-7a is thought to be a tumor suppressor that inhibits the malignant growth of cancer cells by reducing RAS and HMGA2 expression. Reduced expression levels of let-7 have been observed in colon, lung, ovary, and breast cancer cells.[3] Therefore, miRNA replacement therapies have emerged as promising treatment strategies for malignant neoplasms. Yet although miRNA-based modalities may eventually prove effective, their clinical application has been hampered by a lack of appropriate delivery systems.

Exosomes or microvesicles are small vesicles (50–100 nm in diameter) that are secreted by a variety of cell types and tissues.[4] Of clinical interest, tumor cells have been shown to release exosomes containing miRNA[5] and miRNAs secreted from donor cells can be taken up and function in recipient cells.[6,7] These data indicate that exosomes are natural carriers of miRNA that could be exploited as an RNA drug delivery system. For instance, Alvarez-Erviti *et al.* recently used exosomes with modified membranes containing a neuron-specific peptide to deliver small-interfering RNA (siRNA) to mouse brain tissue.[8] Nevertheless, the utility of exosomes as carriers of cancer therapies remains largely unknown.

A number of human tumors of epithelial origin display elevated epidermal growth factor receptor (EGFR) expression, suggesting that EGFR could serve as a receptor target in cancer drug delivery systems.[9] Because the EGFR ligand epidermal growth factor (EGF) is strongly mitogenic and neoangiogenic, however, an alternative ligand is needed for clinical applications.

The GE11 peptide (amino-acid sequence YHWYGYTPQNVI) binds specifically to EGFR, but is markedly less mitogenic than EGF.[10] Additionally, GE11-conjugated polyethylenimine vectors and polyethylene glycol–conjugated liposomes have been shown to be less mitogenic, and can efficiently transfect genes into cells expressing high levels of EGFR or tumor xenografts.[10–13] These studies indicated that the GE11 peptide is likely superior to EGF for clinically targeting EGFR-expressing tumors.

In this study, we examined exosomes as drug delivery carriers in a model of cancer. Modified exosomes with the GE11 peptide or EGF on their surfaces delivered miRNA to EGFR-expressing cancer tissues; intravenously injected exosomes targeting EGFR delivered let-7a specifically to xenograft breast cancer cells in RAG2$^{-/-}$ mice. These data indicate that exosomes targeted to EGFR-expressing cells may provide a platform for miRNA replacement therapies in the treatment of various cancers.

RESULTS

GE11- and EGF-positive exosomes

GE11 peptide specifically binds to EGFR, but is less mitogenic than EGF.[10] To generate GE11- or EGF-positive exosomes, sequence encoding GE11 or EGF was cloned into the pDisplay vector. This vector promotes the expression of proteins on plasma membranes

Correspondence: Masahiko Kuroda, Department of Molecular Pathology, Tokyo Medical University, 6-1-1 Shinjuku, Shinjuku-ku, Tokyo 160-8402, Japan. E-mail: kuroda@tokyo-med.ac.jp

using the transmembrane domain of platelet-derived growth factor receptor (**Figure 1a**). We transfected human embryonic kidney cell line 293 (HEK293) cells with pDisplay encoding GE11 or EGF, and then cloned cells that were stably expressing the constructs. Exosomes were purified from culture supernatants using an ultracentrifugation protocol (see Materials and Methods section).

We then examined the expression of GE11 or EGF in exosomes using anti-hemagglutinin (HA) antibodies and western blot analysis, which revealed bands of the predicted sizes (**Figure 1b**). In addition, fluorescence-activated cell sorting (FACS) confirmed the presence of GE11 and EGF on the outer membranes of exosomes bound to latex beads, and these complexes were recognized by anti-Myc-tag antibodies (**Figure 1c**). CD81 was used as a positive control for exosomes. Myc-tag expression was observed more frequently in EGF-positive (73.8%) and GE11-positive (66.2%) exosomes than in vector control (14.3%) exosomes. These data indicated that GE11 or EGF was present on the exosomal membranes. Additionally, immunogold staining with anti-HA antibodies showed that 15.3% and 21.2% of the exosomes were positive for GE11 and EGF, respectively, and no notable morphologic abnormalities were observed in the modified exosomes (**Figure 1d**).

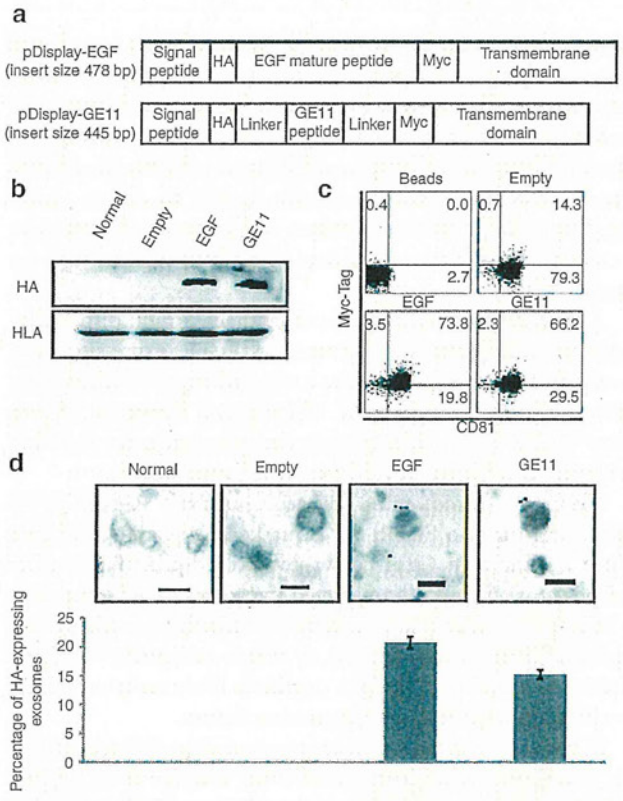

Figure 1 Epidermal growth factor receptor (EGFR) ligands on the outer surfaces of the exosomes. (**a**) Diagrams of the modified epidermal growth factor (EGF) and GE11 proteins. Signal peptide, Igκ-chain leader sequence; HA, hemagglutinin epitope tag (YPYDVPDYA); Linker, (GGGGS) 3; Myc, Myc epitope (EEKLISEEDL); platelet-derived growth factor receptor (PDGFR) transmembrane domain, transmembrane domain from platelet-derived growth factor receptor. (**b**) Western blots of HA-tagged constructs in exosomes obtained from culture supernatants of human embryonic kidney cell line 293 (HEK293) cells that had been transfected with pDisplay encoding EGF or GE11. The quality of each exosome preparation was confirmed by hybridization with antihuman leukocyte antigen (HLA) antibodies. (**c**) For flow cytometry, exosomes from transfected HEK293 cells were incubated with latex beads and stained with anti-Myc tag antibodies. Tetraspanin CD81 was used as a positive control for the exosomes. (**d**) Immunoelectron microscopy showed that HA-tagged constructs were present on exosomes purified from the supernatants of cells transfected with pDisplay encoding EGF or GE11. Bars = 100 nm. The percentages of HA-positive exosomes are indicated in the graph. Data are expressed as means ± SD.

EGFR-dependent uptake of modified exosomes *in vitro*

We next examined whether the GE11- or EGF-positive exosomes derived from HEK293 cells bound to recipient cells in an EGFR-dependent manner. We first evaluated EGFR expression in three human breast cancer cell lines. HCC70 cells showed higher EGFR expression levels than HCC1954 and MCF-7 cells (**Figure 2a**). To examine whether GE11- or EGF-positive exosomes were taken up by recipient cells, exosomes were labeled with PKH67 dye (green) and added to cultures of HCC70 cells (**Figure 2b**). EGF- and GE11-positive exosomes more efficiently bound to HCC70 cells than HCC1954 or MCF-7 cells. Binding appeared to reflect EGFR expression levels (**Figure 2b**). Exosomes did not bind to cell surface membranes when the samples were incubated at 4 °C, suggesting that the cells had to be biologically active (**Figure 2b**). Confocal laser-scanning microscopy demonstrated that the exosomes were internalized by the cells (**Figure 2c**). To confirm that EGF- and GE11-positive exosomes were taken up by an EGFR-dependent mechanism, we performed assays using breast cancer cell lines with different levels of EGFR expression. First, we prepared MCF-7 cells expressing high levels of EGFR using a retroviral vector (**Figure 2d**) and examined uptake of EGF- and GE11-positive exosomes (**Figure 2e**). EGF- and GE11-positive exosomes showed high affinities for these MCF-7 cells compared with cells infected with empty vector or untreated cells. Next, we prepared HCC70 cells in which EGFR expression was knocked down using siRNA. Three days post-transfection, EGFR expression was markedly reduced, and we examined exosome uptake using fluorescence-activated cell sorting analysis (**Figure 2f**). Because the cells proliferated following transfection of EGFR siRNA, relatively low levels of siRNA were detected in PKH67-labeled exosomes compared with the experiment shown in **Figure 2b**. Of note, however, siRNA levels decreased to near background levels in HCC70 cells in which EGFR expression was reduced compared with cells expressing high levels of EGFR or cells transfected with nontarget siRNA.

To assess whether EGF- or GE11-positive exosomes affected cell growth *in vitro*, we performed cell proliferation assays using HCC70 cells. EGF-positive exosomes promoted cell proliferation, whereas no effect was noted with control or GE11-positive exosomes (**Supplementary Figure S1**). These experiments suggested that, unlike EGF-positive exosomes, GE11-positive exosomes do not stimulate EGFR signaling. Thus, GE11-positive exosomes may provide a more suitable drug delivery system than EGF-positive exosomes.

GE11-positive exosomes are functional *in vitro*

Our results indicated that the modified exosomes were taken up into recipient cells. Next, we investigated exosome-mediated delivery of siRNA or miRNA *in vivo*, including the effects of the exogenous siRNA or miRNA in the recipient cells. We first

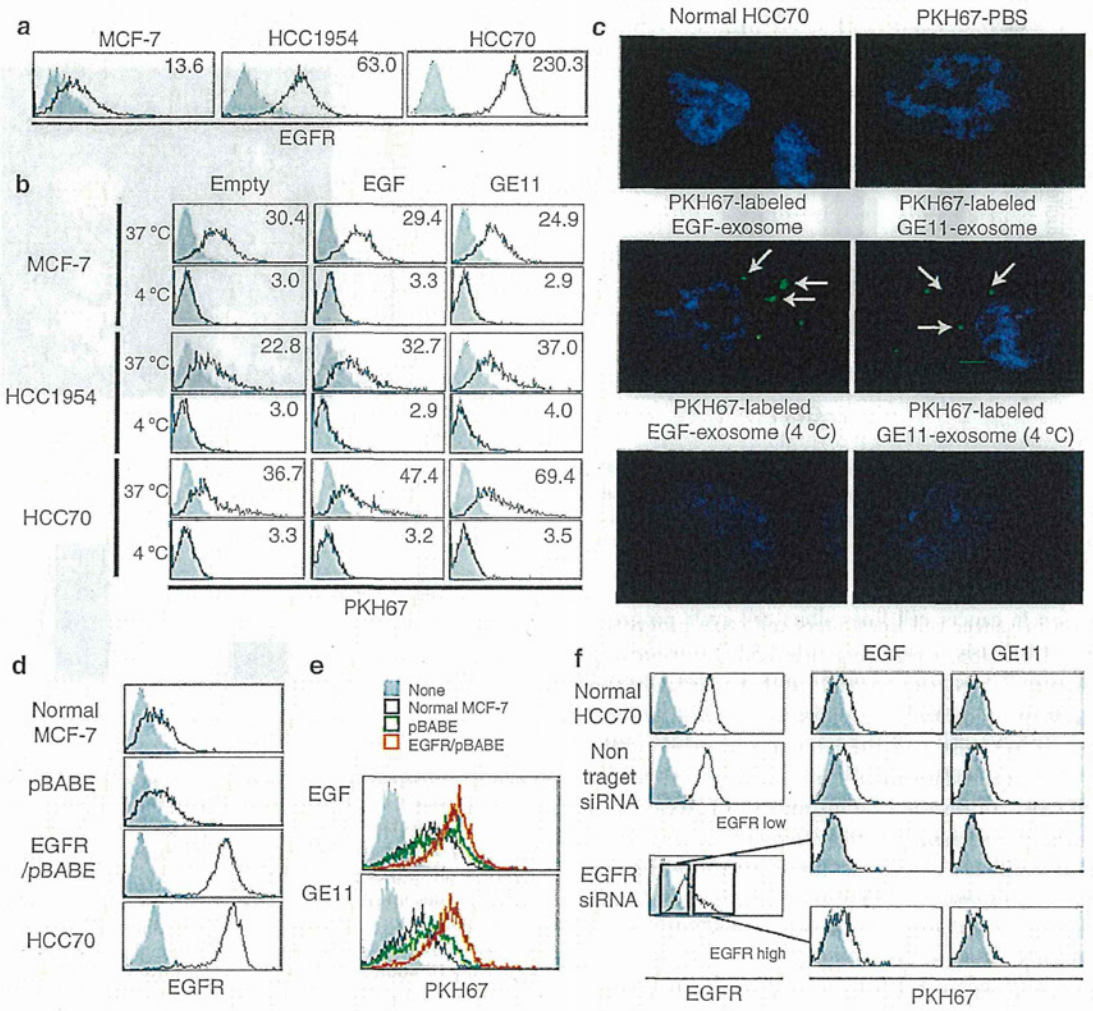

Figure 2 Uptake of epidermal growth factor (EGF)- and GE11-positive exosomes by breast cancer cell lines. (**a**) Flow cytometric analysis of epidermal growth factor receptor (EGFR) expression on HCC70, HCC1954, and MCF-7 breast cancer cells. (**b**) Uptake of fluorescently labeled exosomes by the breast cancer cell lines was detected using flow cytometry. PKH67-labeled exosomes were incubated with the breast cancer cell lines at 37 °C or 4 °C for 4 hours. The degree of uptake was relatively low at 4 °C. (**c**) Intracellular PKH67-labeled exosomes were detected in HCC70 cells (arrows) using confocal fluorescence microscopy. (**d**) Flow cytometric analysis of EGFR expression on MCF-7 cells, which were stably infected with retrovirus expressing EGFR. (**e**) Uptake of PKH67-labeled EGF- and GE11-positive exosomes was compared using MCF-7 cells expressing high levels of EGFR and control cells. (**f**) Uptake of PKH67-labeled EGF- and GE11-positive exosomes was compared among $EGFR^{Low}$ HCC70, $EGFR^{High}$, and control cells.

transfected HEK293 cells with luciferase-specific siRNA and purified loaded exosomes. Then, we added the exosomes to culture medium containing luciferase-expressing HCC70 cells. After 24 hours, we measured luciferase activities and found that GE11-positive exosomes containing luciferase-specific siRNA reduced luciferase activity in the cells (**Figure 3**). These exosomes likely contained only a fraction of the transfected siRNA from the exosome-secreting cells. Nevertheless, the encapsulated siRNA significantly inhibited expression of the target luciferase gene.

GE11-positive exosomes bind tumor cells *in vivo*

We then examined whether GE11-positive exosomes specifically bind to tumors *in vivo*. Luciferase-expressing HCC70 cells were transplanted into the mammary fat pads of $RAG2^{-/-}$ mice. GE11-positive and control exosomes were labeled with XenoLight DiR and intravenously injected into tumor-bearing $RAG2^{-/-}$ mice via the tail vein. Twenty-four hours later, the locations of the exosomes were monitored using an *in vivo* imaging system (IVIS). Signals from the GE11-positive exosomes were detected in the xenograft tumors, whereas little signal was detected in experiments using control exosomes (**Figure 4a**). We also counted the exosomes and observed that, compared with control exosomes, three times as many GE11-positive exosomes reached the tumor (**Figure 4b**). In addition, we did not histologically detect any major organ damage in the injected mice (**Supplementary Figure S2**). These data indicated that GE11-positive exosomes may facilitate the delivery of therapeutic molecules to EGFR-expressing tumors *in vivo*.

GE11-positive exosomes containing let-7 inhibit tumor development *in vivo*

We next investigated the delivery of miRNA to tumors using the GE11-positive exosomes. We used let-7a because elevated

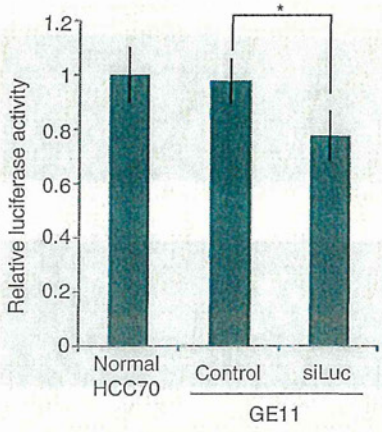

Figure 3 The activity of encapsulated small-interfering RNA (siRNA) in luciferase assays. Luciferase-specific siRNA (siLuc) was encapsulated in exosomes, which were incubated for 48 hours with HCC70 cells stably expressing firefly luciferase. Data are expressed as means ± SD. $n = 3$; $^*P < 0.05$.

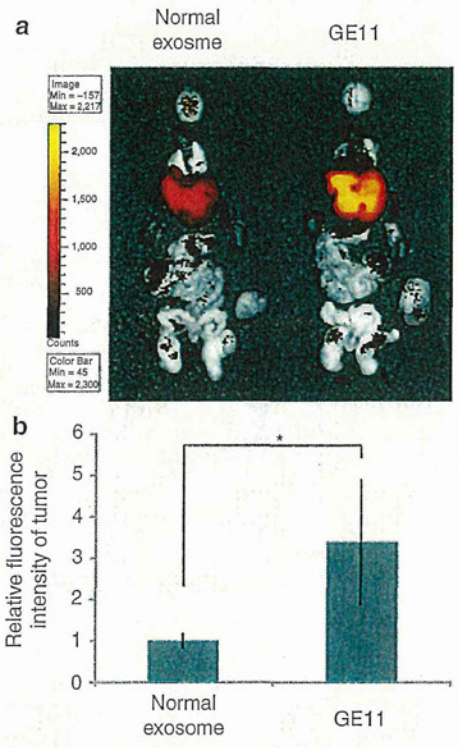

Figure 4 Migration of GE11-positive exosomes to tumor tissues characterized by high levels of epidermal growth factor receptor (EGFR) expression. (a) Exosomes labeled with XenoLight DiR (near-infrared) were intravenously injected (4 μg of purified exosomes) into mice bearing transplanted HCC70 cells. Brain, heart, spleen, liver, lung, kidney, small intestine, colon, and tumor tissues were harvested 24 hours postinjection for *ex vivo* imaging. The migration of fluorescently labeled exosomes was detected with an *in vivo* imaging system (IVIS). **(b)** The intensity of fluorescent signals from the tumor was measured using an IVIS. Data are expressed as means ± SD. $n = 5$; $^*P < 0.05$.

let-7 expression in cancer cell lines alters cell cycle progression and reduces cell division, suggesting that let-7 functions as a tumor suppressor.[14,15] Let-7a or control miRNA was introduced into GE11-positive or control exosomes using the lipofection method and HEK293 cells, and the amount of loaded miRNA was determined in quantitative real-time reverse transcription-PCRs (**Figure 5a**). To measure tumor growth in RAG2$^{-/-}$ mice, we prepared tumor-bearing mice with xenograft HCC70 cells that stably expressed luciferase. To analyze tumor growth and development, we injected the tumors with luciferin and monitored signal emission using an IVIS. Exosomes were intravenously injected into tumor-bearing mice via the tail vein. After four injections, tumor growth was measured. Let-7a–containing GE11-positive exosomes markedly suppressed tumor growth (**Figure 5b** and **c**; $n = 6$, $P < 0.01$). Several studies have reported that let-7a inhibits tumor development by reducing expression levels of HMGA2 or members of the RAS family (K-RAS, H-RAS, N-RAS).[16] We examined the expression of these genes in let-7a–transfected HCC70 cells using real-time reverse transcription-PCR analysis, immunoblotting, and immunostaining (**Supplementary Figure S3a–c**). Furthermore, we immunohistochemically assessed the expression of HMGA2 and RAS family members in xenograft tumors (**Supplementary Figure S3d**). Let-7a did not affect the expression of HMGA2 or RAS family members *in vivo* or *in vitro*. Consistent with previous reports, however, let-7a potently inhibited the expression of HMGA2 mRNA in A549 lung adenocarcinoma cells[17] (**Supplementary Figure S3a**). These data indicated that let-7a inhibits tumor development via previously unidentified or uncharacterized genes in HCC70 breast cancer cells. Taken together, these findings indicated that GE11-positive exosomes are a promising vehicle for delivering drugs to EGFR-expressing tumors.

DISCUSSION

Although miRNA is a promising anticancer therapeutic modality, the clinical use of these RNA molecules has been hampered by a lack of malignant tissue–specific delivery systems. In the present study, we showed that exosomes can be used to efficiently deliver antitumor miRNA to cancer tissues *in vivo*.

A number of nanocarriers using various materials have been developed for drug delivery systems. Polyethylene glycol–coated liposomes, which are frequently used as carriers for *in vivo* drug delivery, benefit from easy preparation techniques, acceptable toxicity profiles, and a lack of clearance by the reticuloendothelial system. Liposomes, however, have several drawbacks, including the efficiency of targeting and issues associated with accelerated blood clearance.[18] Although exosomes and liposomes have similar phospholipid bilayers, exosomes consist of only biogenic substances. The potential of exosomes as drug delivery carriers, however, is largely unknown. Adding appropriate targeting molecules can cause exosomes to accumulate at sites of disease *in vivo* (ref. 7 and **Figure 4**). Thus, the biocompatibility and toxicity profiles of exosomes, which notably are natural carriers of miRNA *in vivo*, support their application in drug delivery systems.

To use exosomes clinically, however, further studies are needed to resolve several issues. For instance, therapeutic exosomes should not be quickly cleared by the reticuloendothelial system. In this study, when fluorescently labeled exosomes were injected into the mice tail vein, many exosomes accumulated

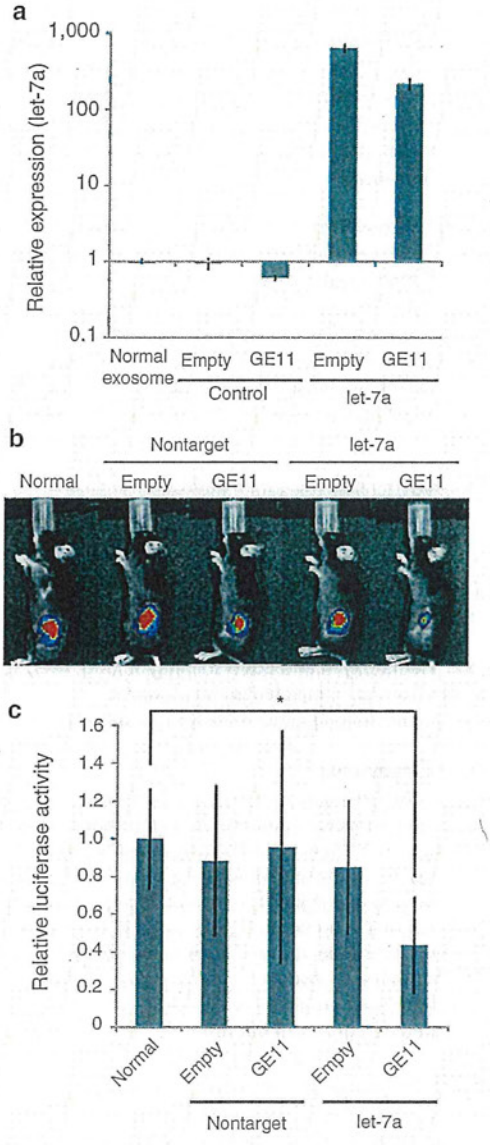

Figure 5 Inhibition of breast cancer development *in vivo* using GE11-positive exosomes containing let-7a. Human embryonic kidney cell line 293 (HEK293) cells expressing GE11 were transfected with synthetic let-7a. Exosomes containing let-7a were purified from culture supernatants and intravenously injected (1 µg of purified exosomes, once per week for 4 weeks) into mice bearing luciferase-expressing HCC70 cells. (**a**) Let-7a levels in the purified exosomes were measured using quantitative PCRs. Data are expressed as means ± SD. $n = 3$. (**b**) Representative images of tumors 4 weeks postinjection are shown. (**c**) Luciferase signals from the tumors were measured using an *in vivo* imaging system (IVIS). Data are expressed as means ± SD. $n = 5$; $^*P < 0.05$.

in the liver 24 hours after the injection (**Figure 4a**). Thus, some modifications are required to avoid normal clearance mechanisms.

This type of delivery strategy requires that the miRNA or siRNA can be efficiently introduced into the exosomes. We transfected donor cells with miRNA and purified exosomes from the culture supernatant. A previous report described electroporation protocols for loading siRNA into exosomes.[8] We, however, were unable to use these methods to load our exosomes with miRNA. The differences in the results may have been caused by the different cell types that were used in the two studies.

The composition of exosomes appears to differ depending on the source tissue or cell type. For instance, major histocompatibility complex class II molecules are enriched in exosomes from B lymphocytes, dendritic cells, mast cells, and intestinal epithelial cells, whereas higher levels of growth factors and their receptors are found in exosomes released from cancer cells.[19] For allogeneic exosome therapy, the presence of major histocompatibility complex proteins is problematic owing to potential immune responses. Therefore, the appropriate selection of donor cells for exosome production is a key factor for potential clinical applications of exosome-based therapies.

In conclusion, exosomes targeted to tumors may allow systemic administration of miRNA as cancer therapy. Technologic improvements that enhance exosome production and reduce immunogenicity should be explored to further develop this drug delivery approach.

MATERIALS AND METHODS

Plasmids transfection and retrovirus infection. The pDisplay vector was purchased from Invitrogen (Carlsbad, CA). Sequence encoding GE11 peptide (YHWYGYTPQNVI) with a flexible peptide linker (GGGGS)3 or mature EGF (53 amino acids, GenBank accession number P01133) was directly fused into pDisplay (**Figure 1a**). HEK293 cells were transfected with pDisplay encoding GE11 or EGF using FuGENE HD transfection reagent (Promega, Madison, WI) and selected with Geneticin (Invitrogen).

EGFR retroviral vector was purchased from Addgene (Cambridge, MA). Viral supernatants were produced by transient transfection of GP2-293T cells with a packaging plasmid (pVSV-G) according to the manufacturer's instructions (Clontech, Mountain View, CA). MCF-7 cells were infected with viral supernatants using polybrene at a final concentration of 8 µg/ml.

Cell culture and small RNA transfection. Breast cancer cell lines (HCC70, HCC1954, and MCF-7) and a HEK293 were purchased from the American Type Culture Collection (Manassas, VA). Cells were cultured according to the manufacturer's instructions. HCC70 cells express firefly luciferase, as previously described.[20] miRNA and siRNA used in this study were as follows: has-let-7a sense (5′-UGAGGUAGUAGGUUGUAUAGUU-3′) and antisense (5′-CUAUACAAUCUACUGUCUUUC-3′); nontarget control miRNA sense (5′-AUCCGCGCGAUAGCACGUAUU-3′) and antisense (5′-UACGUACUAUCGCGCGGAUUU-3′); EGFR-specific siRNA sense (5′-GUGAGGUGGUCCUUGGGAATT-3′) and antisense (5′-UUCCC AAGGACCACCUCACTT-3′); luciferase-specific siRNA sense (5′-CUU ACGCUGAGUACUUCGATT-3′) and antisense (5′-UCGAAGUACUCA GCGUAAGTT-3′); and nontarget control siRNA sense (5′-AUCCGCGC GAUAGCACGUATT-3′) and antisense 5′-UACGUACUAUCGCGCGGA UTT-3′). Oligonucleotides were transfected into cells using HiPerFect reagent (final concentration, 50 nmol/l; Qiagen, Hilden, Germany) according to the manufacturer's instructions.

Western blot analysis. Western blot analysis was performed as previously described.[21] Exosome samples were lysed in sodium dodecyl sulfate loading buffer. After boiling, equal amounts (4 µg) of the proteins were electrophoresed on 15% sodium dodecyl sulfate-polyacrylamide gels and transferred to Immobilon membranes (Millipore, Bedford, MA) using semidry blotting. Then, using standard techniques, the membranes were probed with antibodies, including anti-HA (HA7) (Sigma-Aldrich, St Louis, MO) and anti-HLA-A/B/C (H-300) (Santa Cruz Biotechnology, Santa Cruz, CA). Labeling was visualized using Immobilon Western chemiluminescent

horseradish peroxidase substrate (Millipore) and signals were examined on an LAS-3000 mini system (Fujifilm, Tokyo, Japan).

RNA isolation and quantitative real-time reverse transcription-PCRs. RNA was isolated from exosomes using Isogen reagent (Nippon Gene, Osaka, Japan) according to the manufacturer's instructions. miRNA levels were quantified using TaqMan miRNA assays (Applied Biosystems, Carlsbad, CA). Copy numbers were calculated based on a standard curve created using synthetic RNA. miRNA levels were normalized based on has-miR-16 levels. Quantitative PCRs were run on a Stratagene MX3000P thermocycler and analyzed with MxPro (Agilent Technologies, Santa Clara, CA).

Preparation of exosomes. Exosomes were prepared from HEK293 cells that had been cultured for 48 hours in Dulbecco's modified eagle medium supplemented with 1% GlutaMax (Invitrogen). Cell supernatants were subjected to differential centrifugation. To eliminate cellular debris, samples were centrifuged at 2,000*g* for 20 minutes and 10,000*g* for 30 minutes. Exosomes were pelleted via ultracentrifugation at 120,000*g* for 70 minutes and washed once in phosphate-buffered saline. Protein content in the exosomes was measured using a Protein Assay Rapid Kit (Wako Pure Chemicals, Osaka, Japan). The average exosome yield was 69.2 μg from 100 ml (2–5 × 10^7 cells) of culture supernatant ($n = 8$).

Flow cytometry. For fluorescence-activated cell sorting, exosomes from HEK293 cells were adsorbed onto 4-μm aldehyde-sulphate latex beads (Interfacial Dynamics, Tualatin, OR), incubated with Alexa Fluor 488–conjugated anti-Myc tag antibodies (Millipore, Temecula, CA) or allophycocyanin-conjugated anti-CD81 antibodies (BD Pharmingen, San Jose, CA), and analyzed on a FACSCalibur system (Becton Dickinson, San Diego, CA).

Immunoelectron microscopy. Purified exosomes from HEK293 cells were fixed in 2% paraformaldehyde and loaded onto Formvar-coated Ni electron microscopy grids. The samples were incubated overnight at 4 °C with anti-HA antibodies (Sigma-Aldrich) followed by 1 hour at room temperature with anti-mouse immunoglobulin G conjugated with 15-nm colloidal gold particles. The samples then were fixed in 2% glutaraldehyde, stained with 1% phosphotungstic acid, air-dried, and analyzed using a Hitachi H-7000 electron microscope (Hitachi High-Technologies, Tokyo, Japan). Exosomes positive or negative for gold particles were counted in 10 grids (~1,000–2,000 exosomes).

Coculture of PKH67-labeled exosomes and breast cancer cell lines. Exosomes were stained with green PKH67 fluorescent dye (Sigma-Aldrich). After staining, exosomes were washed with phosphate-buffered saline and centrifuged at 120,000*g* for 70 minutes. One microgram of PKH67-labeled exosomes was incubated with 1 × 10^5 breast cancer cells at 37 °C or 4 °C for 4 hours. The uptake of PKH67-labeled exosomes was analyzed using flow cytometry and confocal fluorescence microscopy.

Administration of let-7a–containing exosomes in a human tumor xenograft model. Luciferase-expressing HCC70 cells (2 × 10^6) were injected subcutaneously into the mammary fat pads of 5-week-old RAG2$^{-/-}$ mice. Four weeks after transplantation, tumors were sized using an IVIS (Xenogen, Hopkinton, MA). HEK293 cells expressing GE11 were transfected with synthetic let-7a. Let-7a–containing exosomes were purified from culture supernatants and intravenously injected (1 μg of purified exosomes, once per week for 4 weeks) into mice with transplanted luciferase-expressing HCC70 cells. Let-7a levels in the exosome samples were evaluated using TaqMan miRNA assays and real-time PCRs. Mice were handled according to the Ethical Guidelines of our institution. All experiments were approved by the Committee for Animal Research at our institution.

In vivo *imaging of fluorescently labeled exosomes.* A stock solution of the lipophilic near-infrared dye XenoLight DiR (Caliper Life Sciences, Hopkinton, MA) was prepared in ethanol. A 300-μmol/l working solution was prepared in diluent-C solution (Sigma-Aldrich). Exosomes isolated from culture supernatant–derived HEK293 cells were incubated with 2 μmol/l DiR for 30 minutes. The exosomes were then washed with 10 ml of phosphate-buffered saline, subjected to ultracentrifugation, and injected intravenously into RAG2$^{-/-}$ mice (4 μg of exosomes/mouse). Migration of fluorescently labeled exosomes in murine organs was detected using an IVIS 24 hours postinjection.

In vivo *imaging of xenograft tumors.* Mice were anesthetized via isoflurane inhalation, and intraperitoneally injected with 100 μl of 7.5 mg/ml luciferin solution (Promega). Bioluminescence imaging was initiated with an IVIS (Xenogen) 10 minutes postinjection. The region of interest was defined manually, and bioluminescence data are expressed as photon flux values (photons/s/cm²/steradian). Background photon flux was defined using an area of the tumor that did not receive an intraperitoneal injection of luciferin. All bioluminescence data were collected and analyzed using an IVIS.

Statistical analysis. Differences were statistically evaluated using one-way analysis of variance followed by the Fisher protected least significant difference test. P values <0.05 were defined as statistically significant.

SUPPLEMENTARY MATERIAL

Figure S1. Analysis of cell viability based on assays with (4, 5-dimethylthiazol-2-yl) 2,5-diphenyl-tetrazolium bromide.
Figure S2. Hematoxylin and eosin staining of lung, liver, spleen, and kidney tissues from mice injected with exosomes.
Figure S3. Expression analysis of the let-7 target genes.

ACKNOWLEDGMENTS

This work was done in Shinjyu-ku, Tokyo, Japan. This work was supported by the "Private University Strategic Research-Based Support Project: Epigenetics Research Project Aimed at a General Cancer Cure Using Epigenetic Targets" from the Ministry of Education, Culture, Sports, Science and Technology (MEXT) of Japan and in part by a grant-in-aid for scientific research on PriorityAreas (B) and (C) from MEXT (Japan) and the Tokyo Medical University Cancer Research Foundation (Japan). We are also indebted to Roderick J. Turner, Edward F. Barroga, and J. Patrick Barron for their editorial review of the English manuscript. The authors declared no conflict of interest.

REFERENCES

1. Bartel, DP (2004). MicroRNAs: genomics, biogenesis, mechanism, and function. *Cell* **116**: 281–297.
2. Calin, GA and Croce, CM (2006). MicroRNA signatures in human cancers. *Nat Rev Cancer* **6**: 857–866.
3. Barh, D, Malhotra, R, Ravi, B and Sindhurani, P (2010). MicroRNA let-7: an emerging next-generation cancer therapeutic. *Curr Oncol* **17**: 70–80.
4. Lotvall, J and Valadi, H (2007). Cell to cell signalling via exosomes through esRNA. *Cell Adh Migr* **1**: 156–158.
5. Skog, J, Würdinger, T, van Rijn, S, Meijer, DH, Gainche, L, Sena-Esteves, M *et al.* (2008). Glioblastoma microvesicles transport RNA and proteins that promote tumour growth and provide diagnostic biomarkers. *Nat Cell Biol* **10**: 1470–1476.
6. Akao, Y, Iio, A, Itoh, T, Noguchi, S, Itoh, Y, Ohtsuki, Y *et al.* (2011). Microvesicle-mediated RNA molecule delivery system using monocytes/macrophages. *Mol Ther* **19**: 395–399.
7. Kosaka, N, Iguchi, H, Yoshioka, Y, Takeshita, F, Matsuki, Y and Ochiya, T (2010). Secretory mechanisms and intercellular transfer of microRNAs in living cells. *J Biol Chem* **285**: 17442–17452.
8. Alvarez-Erviti, L, Seow, Y, Yin, H, Betts, C, Lakhal, S and Wood, MJ (2011). Delivery of siRNA to the mouse brain by systemic injection of targeted exosomes. *Nat Biotechnol* **29**: 341–345.
9. Woodburn, JR (1999). The epidermal growth factor receptor and its inhibition in cancer therapy. *Pharmacol Ther* **82**: 241–250.
10. Li, Z, Zhao, R, Wu, X, Sun, Y, Yao, M, Li, J *et al.* (2005). Identification and characterization of a novel peptide ligand of epidermal growth factor receptor for targeted delivery of therapeutics. *FASEB J* **19**: 1978–1985.
11. Song, S, Liu, D, Peng, J, Sun, Y, Li, Z, Gu, JR *et al.* (2008). Peptide ligand-mediated liposome distribution and targeting to EGFR expressing tumor in vivo. *Int J Pharm* **363**: 155–161.
12. Klutz, K, Schaffert, D, Willhauck, MJ, Grünwald, GK, Haase, R, Wunderlich, N *et al.* (2011). Epidermal growth factor receptor-targeted (131)I-therapy of liver cancer following systemic delivery of the sodium iodide symporter gene. *Mol Ther* **19**: 676–685.